

RESEARCH
ENGINEERING
PRODUCTION

83p.

N64-19625

CODE-1

NASA CR-53633



OTS PRICE

XEROX \$ 8.10 ph
MICROFILM \$ 2.69 mf.

GENERAL APPLIED SCIENCE LABORATORIES, INC.
MERRICK and STEWART AVENUES, WESTBURY, L.I., N.Y. (516) ED 3-6960

548-13290

Copy No. (7) of (2)

Total No. Pages:

126 / THE LAMINAR BOUNDARY LAYER
IN HYDROGEN-AIR MIXTURES
WITH FINITE RATE CHEMISTRY

TECHNICAL REPORT NO. 385

→ P. A. Libby, H. Rosenbaum, and S. Slutsky

(NASA Contract No. NAS8-2686)

Prepared for

National Aeronautics and Space Administration
George C. Marshall Space Flight Center
Huntsville, Alabama

(NASA CR-53633) OTS:

#8.10 pl, 2.07

Prepared by

[8]

General Applied Science Laboratories, Inc.,
Merrick and Stewart Aves.
Westbury, L.I., New York

102 4652

November 1963, 83p ref

Approved by: Antonio Ferri / 38
Antonio Ferri
President

TABLE OF CONTENTS

I	Introduction	1
II	Idealization of the Flow	4
III	Analysis	7
IV	Calculations	25
V	Results and Conclusions	27
VI	List of Symbols	31
VII	References	32
	Appendix I	35
	Appendix II	44

ABSTRACT

19625

A

There is presented herein an analysis of the compressible laminar boundary layer with an external stream of air of uniform velocity and with hydrogen fuel present in the flow. The transport processes have been simplified by considering the $p\mu$ product at each streamwise station to be independent of the normal coordinate and by assuming all Prandtl and Lewis numbers equal to unity. Finite rate chemistry is treated in detail. Nitrogen was assumed to be an inert diluent and eight forward and eight reverse reaction steps of the hydrogen-oxygen system have been employed. An implicit finite difference method of solution has been developed. Numerical solutions for diffusive flows are presented but difficulty was encountered in cases of energetic chemical reaction.

Author

THE LAMINAR BOUNDARY LAYER IN HYDROGEN-AIR MIXTURES WITH FINITE RATE CHEMISTRY

I INTRODUCTION

As part of a study of the problems connected with the dumping of a fuel such as hydrogen from the upper stages of an exiting boost vehicle, there are considered here the characteristics of the laminar boundary layers in a hydrogen-air mixture with finite rate chemistry. The problem being treated may be of some interest not only for the immediate application cited above but also for its fundamental significance. Laminar boundary layers in chemically reacting flows have been of increasing importance in recent years; References 1-10 provide some indications of the current status of the theory thereof.

In most of these studies two classes of approximations are applied beyond those associated with boundary layer theory. These pertain to simplified transport of mass, momentum and energy and to simplified chemical kinetics. These approximations are generally considered necessary in order to reduce to tractable levels the numerical difficulties associated with solution of the describing equations. Thus the product of mass density and viscosity is generally taken to be constant and the Prandtl number and Lewis numbers are taken to be unity. Until recently these approximations have been considered not to obscure the essential features of the phenomena. However, as noted in the following these parameters may vary strongly across a multi-component boundary layer. The treatment of the chemical behavior is usually carried out in terms of either of the two limiting cases: "very slow" chemical reaction corresponding to frozen flow or "very fast" chemical reaction corresponding to equilibrium flow. This treatment does not provide,

except in terms of "order of magnitude" considerations, any indication of which of these two cases is likely to prevail in a given flow. Thus the question of whether combustion does or does not take place within the boundary layer is not answered by analyses of the limiting cases and essential features of the phenomena are lost.

There have been several analyses of laminar flows of the boundary layer type with finite rate chemistry. Marble and Adamson (Reference 7) considered the ignition of a combustible gas by laminar mixing; Dooley (Reference 8) applied the same approach to the boundary layer on a heated flat plate. In both of these studies a one-step chemical reaction was considered; an iterative method of solution of the species equation was employed. Chung and Anderson (Reference 9) have treated the dissociation of a diatomic gas in a high speed flow with finite rates; an integral method of solution was employed. Finally, finite rate chemistry for air has been applied to hypersonic wake flows by Vaglio-Laurin and Bloom (cf., e.g., Reference 10).

It is the purpose of the present report to provide an analysis of the laminar boundary layer with an external stream of uniform velocity and with a fuel present in the flow. Several remarks concerning the point of view taken in the study presented here are perhaps in order; the general analysis has been set up for an arbitrary fuel-oxidizer system but the detailed treatment and numerical examples have been carried out for the hydrogen-air system with the fuel in gaseous form. The transport processes have been simplified by considering the $\rho\mu$ product at each streamwise station to be independent of the normal coordinate and by assuming all Prandtl and Lewis numbers equal to unity. It will thus be recognized that the frequently employed approximations relative to transport properties are applied here. Finite rate chemistry is considered essential and is treated in detail. An

implicit finite difference method of solution has been selected with the view to provide a "growth capability" for handling in the future more realistic transport processes and flows with non-uniform external flow conditions.

The chemistry of the hydrogen-air system employed in this report follows closely that of References 11 and 12. Thus nitrogen was assumed to be an inert diluent but the reaction steps of the hydrogen-oxygen system, eight forward and eight reverse, following the work of Duff and co-workers (References 13 and 14), have been employed.

The report is organized as follows: The idealization of the flow is discussed first and is followed by a treatment of the momentum and energy equations. The species conservation equations for a general chemical system with simplified transport properties are discussed next, particular attention being directed to the external conditions applicable in various cases. The chemistry of the hydrogen-air system is then described and the general treatment of the species equations related particularly to this chemical system is also described. The details of the finite difference method of solution are given in Appendix II. The report concludes with some numerical results which may be of importance for the hydrogen dumping problem.

The authors gratefully acknowledge the work of Mr. Harry Gould who wrote the finite difference machine program for the I. B. M. 7090 digital computer.

II IDEALIZATION OF THE FLOW

The actual processes which may be considered when a fuel such as hydrogen is ejected from the upper stage of an exiting launch vehicle may be complex. One of the most important practical questions to be considered is whether or not combustion actually occurs under given flight conditions. In Reference 15 an order of magnitude analysis based on flow times for a typical exit trajectory and chemical times based on the hydrogen-air system is presented; it is shown that there is a critical altitude in the range from 125 to 175 kilofeet depending on the mode of dumping where the lengths associated with the initiation of heat release may be relatively short. The analysis of Reference 15 does not include the times associated with the vaporization of fuel in liquid or solid phase and with mixing of fuel and oxidizer; it may thus lead to excessively conservative times associated with combustion. However, this analysis did indicate that either slot injection parallel to the surface of the vehicle or injection from a downstream facing pipe provides an environment for the fuel making it less likely to combust in lengths of practical interest.

The present study is directed toward answering in part the question of whether or not combustion does occur under given flight conditions. To treat this question for a chemical system as complex as that for practical fuels with air as an oxidizer, it is necessary to idealize the flow. The aforementioned result concerning the desirability of slot injection suggests as a model for finite rate chemistry the flow shown schematically in Figure 3. The fuel in gaseous form is injected into the air stream from a slot of height "a" with a velocity u_j equal to that in the external stream, i.e., to u_e . The boundary layers on the walls of the slot and on the splitter

plate are neglected so that effectively a boundary layer grows on the wall of the vehicle starting at the slot exit. The static pressure in the fuel at the slot exit is assumed equal to that in the external stream; indeed the static pressure throughout the flow is taken to be constant so, for example, the velocity in the external stream, u_e , is constant. Finally, the flow is assumed to be laminar, two-dimensional and steady.

The implications of these idealizations with respect to practical flows are in general evident. For example, the neglect of the boundary layers upstream of the slot exit and the assumption of laminar flow imply that such boundary layers are negligibly thin with respect to the slot height "a" and are laminar. * The assumption of uniform pressure implies the non-existence of either shock or expansion waves at the exit of the slot and the absence of interaction between the boundary layer and the external stream due to heat release. Finally, the assumptions of $u_j = u_e$ implies that the initial mixing between fuel and oxidizer occurs at the origin of mixing ($x = 0$, $y = a$) in an isovelocity region. It is noted that some of these assumptions can be relaxed in future studies without undue difficulty provided the flow remains laminar. However, the detailed treatment of turbulent flows with finite rate chemistry poses difficult fundamental problems (cf., e.g., Reference 12).

The idealization of the flow as shown in Figure 1 is supplemented in the present report by simplifying assumptions with respect to the laminar transport processes. In particular the product of mass density and of viscosity coefficient ($\rho \mu$) will be treated as a function of x , i.e., the actual distribution

*This assumption also implies that the flow time required for the boundary layer on the splitter plate to "smooth out" is negligible compared to a chemical reaction time. In future extensions of this work this assumption will be removed.

at each station x will be replaced by an effective value of this product. The Prandtl number will be taken to be constant and equal to unity. Finally, the diffusion coefficient associated with the diffusion of each species in the mixture of all species will be assumed to yield a Lewis number equal to unity. Again it is noted that these assumptions are not essential to the numerical analysis applied here and will be relaxed in future studies.

III ANALYSIS

The idealizations and assumptions described above permit the following approach to be exploited; the describing equations of mass, momentum, energy, element, and species conservation can be transformed to s, η variables where $s=s(x)$ and $\eta = \eta(x, y)$. In these variables the velocity field is given by the usual Blasius solution and can be found prior to the distributions which relate to the stagnation enthalpy, element concentrations, and species concentrations and which are here obtained by finite difference calculations. Effectively then the velocity field is uncoupled with respect to the energy and composition fields.

Velocity Field

Consider the boundary layer on the surface of the vehicle as shown in Figure 1 in a gas flow of arbitrary chemical composition.. The momentum and mass conservation equations according to boundary layer theory are*

$$\rho u \frac{\partial u}{\partial x} + \rho v \frac{\partial v}{\partial y} = \frac{\partial}{\partial y} \left(\mu \frac{\partial u}{\partial y} \right) \quad (1)$$

$$\frac{\partial}{\partial x} (\rho u) + \frac{\partial}{\partial y} (\rho v) = 0 \quad (2)$$

*Note that the analysis will be carried out here explicitly for two-dimensional flow; the extension to axisymmetric flow is straightforward.

It is desired to employ these equations to obtain the characteristics of the velocity field in the boundary layer involving a reacting gas. A general specification of the transport properties, particularly of the product ρu leads to non-similar flows, i.e., those for which no combination of x and y into a new variable yields the complete description of the flow. For the purposes of making engineering estimates it is therefore a great simplification to consider at each station x a mean value of the product ρu ; in this way part of the affect of large changes in this transport parameter are accounted for.

Introduce a new independent variable which is a slight modification of the usual Levy-Lees variable (References 16 and 17), namely

$$\eta = \frac{\rho_e u_e}{\mu_e \sqrt{2S}} \int_0^y \frac{\rho}{\rho_e} dy' \quad (3)$$

where

$$S = \frac{\rho u_e}{\mu_e} \int_0^x \bar{C}(x') dx' \quad (4)$$

and where $\bar{C} = \bar{\rho} \mu / \rho_e \mu_e$, $(\bar{\rho} \mu)$ being some characteristic product of mass density and viscosity considered a function of the streamwise coordinate x . Furthermore, assume the stream function satisfying Equation (2) is of the form

$$\psi(x, y) = \sqrt{2S} f(\eta) \quad (5)$$

where

$$\rho u = \mu_e \frac{\partial \psi}{\partial y} ; \quad \rho v = -\mu_e \frac{\partial \psi}{\partial x}$$

Then provided $C = \bar{C}$ where $C \equiv \rho \mu / \rho_e \mu_e$ Equation (1) becomes the well known Blasius equation

$$f''' + f f'' = 0 \quad (6)$$

which is subject to the boundary conditions

$$f(0) = f'(0) = 0 ; \quad f'(\infty) = 1$$

The parameter of interest is $f''(0) = 0.470$ (cf., e.g., Reference 17).

Energy Equation

Consider next the energy equation written in terms of the stagnation enthalpy h_s ; let the diffusion of each species in the mixture be described by a Fick's law involving a mixture diffusion coefficient, i.e., that

$$\rho_i V_i = -D_{i,m} \frac{\partial Y_i}{\partial y} \quad (7)$$

Assume that the Lewis numbers $\rho D_{i,m} c_p / k \approx 1$, for all i and that the Prandtl number of the mixture is everywhere unity; then the energy equation becomes

$$\rho u \frac{\partial h_s}{\partial x} + \rho v \frac{\partial h_s}{\partial y} = \frac{\partial}{\partial y} \left(\mu \frac{\partial h_s}{\partial y} \right) \quad (8)$$

Now transform the equation to the s, η variable defined by Equations (3) and (4) and introduce the variable $g \equiv h_s / h_{s,e}$; there is obtained

$$\frac{\partial^2 g}{\partial \eta^2} + f \frac{\partial g}{\partial \eta} - 2s f' \frac{\partial g}{\partial s} = 0 \quad (9)$$

The boundary conditions are

$$\begin{aligned} g(s, 0) &= g_w(s) \\ g(s, \infty) &= 1 \end{aligned}$$

At this point in the analysis it is perhaps appropriate to consider the initial conditions which will be imposed on the energy equation, i.e., on Equation (9) and subsequently on the element and species conservation equations. The transformations on the s, η variables do not permit arbitrary initial conditions to be specified at $s = 0$. However, at $s = s_1 > 0$ such conditions can be imposed and can be determined for the flow as idealized in Figure 1 according to the following considerations: Close to the origin of mixing there will exist two distinct viscous regions which will interact with one another only weakly if at all. There is the isovelocity free mixing region originating at the point $x = 0, y = a$, and the wall boundary layer originating in this idealization at $x = y = 0$. The form of these two regions diffuses the stagnation enthalpy and the composition differences existing between the slot and external flows. The wall boundary layer may be considered to grow in gas issuing from the slot, i.e., to be essentially devoid of gas from the external stream. These two viscous regions can be treated more or less independently until at a station $x = x_1$ where

the adjacent "edges" of the two viscous regions approach one another. The distributions of enthalpy and composition at this station provide the initial data for the solution of the energy equation, i.e., for Equation (9), and of the element and species equations which will be discussed below. The detailed discussion of the determination of these initial distributions will be presented in Appendix 1. Consider to complete the formulation of the energy equation an initial profile specified as

$$g(s, \eta) = g_\infty(\eta) \quad (11)$$

It is perhaps worth noting that in a reacting boundary layer the wall enthalpy $h_w = h_{egw}$ is usually not known apriori since the composition at the wall is not known; it is thus more practical to assume a priori a temperature distribution $T_w = T_w(s)$ and to compute $g_w(s)$ as part of the solution.*.

Equation (9) subject to the conditions of Equations (10) and (11) will be solved here by finite difference methods. Since the species conservation equations, which complete the system of partial differential equations, will also be handled by these methods, these equations will now be discussed.

Element Conservation

In the treatment of species conservation it is frequently convenient to utilize the concept of element mass fractions (cf., e.g., References 1, 2, 6, and 19) which define the mass fractions of a particular element in whatever form, i.e., atom, molecule or compound it occurs. The definition of the element mass fractions are

*Note that if $g_w(s)$ is specified a priori an exact solution of Equation (9) subject to its initial and boundary conditions can be obtained (ref. 18). This approach cannot be readily extended and was thus not employed here.

suggested by the statement of element conservation which implies that

$$\sum_{i=1}^N \frac{\mu_{ij} \dot{w}_i}{w_i} \quad (12)$$

where μ_{ij} is the number of atoms of element j in species i . Thus the element mass fractions are defined as

$$\tilde{Y}_j = \frac{\sum_{i=1}^N \mu_{ij} w_i Y_i}{w_i} \quad (13)$$

In view of Equation (12) the conservation equations for the element mass fractions do not involve a creation term; indeed for all Lewis numbers equal to unity the conservation of elements is given by

$$\rho u \frac{\partial \tilde{Y}_i}{\partial x} + \rho v \frac{\partial \tilde{Y}_i}{\partial y} = \frac{\partial}{\partial y} \left(\mu \frac{\partial \tilde{Y}_i}{\partial y} \right) \quad (14)$$

Again transformation to the s, η variable yields for the problem under consideration the equation

$$\frac{\partial^2 \tilde{Y}_i}{\partial \eta^2} + f \frac{\partial \tilde{Y}_i}{\partial \eta} - 2s f' \frac{\partial \tilde{Y}_i}{\partial s} = 0 \quad (15)$$

which is subject to the boundary conditions

$$\begin{aligned} \frac{\partial \tilde{Y}_i}{\partial \eta} (s, 0) &= 0 \\ \tilde{Y}_i (s, \infty) &= \tilde{Y}_{ie} \end{aligned} \quad (16)$$

The initial conditions will be such as those of the stagnation enthalpy, namely

$$\tilde{Y}_i(s, \eta) = \tilde{Y}_{i,s}(\eta) \quad (17)$$

Note that the vanishing of the gradients of the element mass fractions at $\eta = 0$ implies the negligibility of surface reactions; this assumption will be employed here.

The solutions of Equation (15), will be carried out by finite difference methods; indeed it will be noted that the differential operator in Equation (15) is identical to that for the stagnation enthalpy h_s (cf. Equation (9)) although the boundary conditions are different. It should be noted that the desired solutions can be found in closed form (Reference 20). However, these solutions are practical only in terms of non-elementary, i.e., tabulated functions. Moreover, with more realistic transport properties, finite differences must be employed so with a view toward providing "growth capability" in the computer program, the more direct finite difference solutions are employed here.

Species Conservation

The composition is determined in the flow under consideration only when additional species conservation equations are solved. If the flow involves N species with L elements, the $N-L$ species conservation equations must be considered explicitly. Note that if at a generic point in the flow, there are known the L values of the $\tilde{Y}_{i,s}$ and the $N-L$ values of the $Y_{i,s}$ given explicitly by the conservation equations, then the remaining L values of the $Y_{i,s}$ can be found

from the definitions of the element mass fractions, i.e., from Equations (9). In chemical systems of practical interest it is frequently found that the mass fractions at a generic point differ by many orders of magnitude; consequently, this latter step of finding the remaining L mass fractions can lead to degradation in numerical accuracy unless the mass fractions of species present in small amounts are computed from the differential equations, i.e., so that the trace species are among the N-L species given explicitly. *This is possible provided the number of trace species is less than or equal to N-L. If this inequality is not satisfied, then it may be necessary for numerical accuracy to abandon at least in part the conservation equations in terms of the element mass fractions; thus, additional species conservation equations with creation terms must be solved explicitly. Indeed, it is of course possible to consider only species conservation in which case N creation terms must be computed and the element mass fractions are automatically conserved. However, the creation terms are generally complex and involve considerable computation so that use is often made of element mass fractions to reduce the number of such terms.

With the approximation attendant on Equation (7) and with the Lewis numbers all equal to unity, the conservation of a particular species i is described by

$$\rho u \frac{\partial Y_i}{\partial x} + \rho v \frac{\partial Y_i}{\partial y} = \frac{\partial}{\partial y} \left(\mu \frac{\partial Y_i}{\partial y} \right) + \dot{w}_i \quad (18)$$

Again transformation to the s, η variables yields

$$\frac{\partial^2 Y_i}{\partial \eta^2} + f \frac{\partial Y_i}{\partial \eta} - 2s f' \frac{\partial Y_i}{\partial s} + \left(\frac{2s}{c} \right) \left(\frac{\rho_e}{\rho} \right) \left(\frac{\dot{w}_i \mu_e}{\rho_e^2 u_e} \right) = 0 \quad (19)$$

*This suggestion is contained in Reference 21 in connection with inviscid flows but is applicable to diffusive flows as well.

The boundary conditions are

$$\frac{\partial Y_i(s, 0)}{\partial \eta} = 0 \quad ; \quad Y_i(s, \infty) = Y_{ie} \quad (20)$$

Again the initial conditions are

$$Y_i(s, \eta) = Y_{i,0}(\eta) \quad (21)$$

It is interesting to note that in Equation (19) the parameter \bar{C} distorting the streamwise coordinate and the density ρ appear; this is symptomatic of the well-known absence of scaling laws for chemically reacting flows with finite rate chemistry.

Equation (19) subject to the conditions given by Equations (20) and (21) will be solved by finite difference methods.

Auxiliary Equations Related to Static and Transport Properties

The system of conservation equations and their initial and boundary conditions must be supplemented by several auxiliary equations, which will involve the prime dependent variables, f' , g , and the $Y_{i,s}$. In particular the distribution of static temperature will be required; this is implicitly given in terms of the distribution of f' , g and the species mass fractions Y_i according to the definition of g as

$$\sum_i Y_i h_i = h_{se} g - \frac{u_e^2 (f')^2}{2} \quad (22)$$

where $h_i = h_i(T)$. Now for simplicity and yet for accuracy sufficient

for most purposes the relation between the species enthalpy and the temperature can be taken as

$$h_i = \Delta_i + C_{p,i} (T - T_r) \quad (23)$$

Then Equation (18) becomes

$$(T - T_r) = \frac{gh_{se} - (u_e^2/2)(f')^2 - \sum_i Y_i \Delta_i}{\sum_i Y_i C_{p,i}} \quad (24)$$

which yields the temperature explicitly in terms of the prime dependent variables.

For consistence it is noted that

$$(T_e - T_r) = \frac{h_{se} - u_e^2/2 - \sum_i Y_{ie} \Delta_i}{\sum_i Y_{ie} C_{p,i}} \quad (25)$$

Note that the transformation from the s, η plane depends on the availability of the density ratio and that from Equation (3)

$$y = \frac{\mu_e \sqrt{2} s}{\rho_e u_e} \int_0^\eta \frac{\rho_e}{\rho} d\eta' \quad (3a)$$

In addition from Equation (4)

$$x = \frac{\mu_e}{\rho_e u_e} \int_0^s [\bar{C}(s')]^{-1} ds' \quad (4a)$$

which can be employed if $\bar{C}(s)$ is known.

It is necessary to employ the equation of state to determine the mass density ; it is convenient to express

$$\frac{\rho_e}{\rho} = \frac{T}{T_e} \frac{W_e}{W} = \frac{T}{T_e} W_e \sum_{L=1}^N \left(\frac{Y_L}{W_L} \right) \quad (26)$$

The choice of a state for the determination of \bar{C} and the calculation thereof must also be made. At present there appears to be no rational way for determining the parameter which corresponds to the effective $\rho \mu$ product. However, the wall values provide an important and relatively simple state and will be employed here. According to this definition

$$\bar{C} = \frac{\rho_w \mu_w}{\rho_e \mu_e} \quad (27)$$

where ρ_w/ρ_e can clearly be obtained from Equation (26) with $T = T_w$, $W = W_w$, etc.. For μ_w/μ_e , it is necessary to compute the viscosity of gaseous mixtures. The approximate formula given in reference (21) has been employed here; thus,

$$\mu_w = \sum_{i=1}^N \frac{\mu_{i,w} Y_{i,w}}{Y_{i,w} + W_i \sum_{j \neq i} \frac{Y_{j,w}}{W_j} \phi_{ij}} \quad (28)$$

where

$$\phi_{ij} = \frac{\left[1 + \left(\frac{\mu_{i,w}}{\mu_{j,w}} \right)^{1/2} \left(\frac{W_j}{W_i} \right)^{1/4} \right]^2}{\frac{4}{\sqrt{2}} \left[1 + \frac{W_i}{W_j} \right]^{1/2}} \quad (29)$$

A Auxiliary Equations for the Production Terms

The detailed specification of the production terms, i.e., those involving w_i in Equation (19) can only be carried out after the chemical species, their reaction mechanisms, and reaction rates are established. Here the hydrogen-air system with nitrogen treated as an inert diluent will be considered in detail. After References 11-14 the reaction mechanism and rates are taken to be as follows:

<u>Reaction Numbers</u>	<u>Reaction Mechanism</u>	<u>Reaction Rate</u>	
1	$H + O_2 \xrightarrow{k_1} OH + O$	$3 \times 10^{14} e^{-8810/T}$	
2	$O + H_2 \xrightarrow{k_2} OH + H$	$3 \times 10^{14} e^{-4030/T}$	
3	$OH + H_2 \xrightarrow{k_3} H_2O + H$	$3 \times 10^{14} e^{-3020/T}$	
4	$2OH \xrightarrow{k_4} H_2O + H$	$3 \times 10^{14} e^{-3020/T}$	(30)
5	$2H + M \xrightarrow{k_5} H_2 + M$	5×10^{15}	
6	$H + OH + M \xrightarrow{k_6} H_2O + M$	10^{17}	
7	$H + O + M \xrightarrow{k_7} O_2 + M$	10^{16}	
8	$2O + M \xrightarrow{k_8} O_2 + M$	3×10^{14}	

where M denotes any third body; where the units of k_j are (moles/cc)⁻¹ sec⁻¹ for second order reactions proceeding to the right (i.e., reactions 1-4) and (moles/cc)⁻² sec⁻¹ for third order reactions proceeding to the right (i.e., for reactions 5-8); and where T is in °K.

Thus the chemical system involves seven species (N = 7) and three elements (L = 3). It will be convenient to employ a numerical subscript notation to identify

the species; thus let O_2 , H_2 , H_2O , N_2 , O , H , and OH be denoted by the subscripts 1-7 respectively. Thus the elements are denoted by subscripts 1, 2, and 4. The intermediates O , H and OH , are present in trace amounts and may be computed from differential equations of the form of Equation (19) the concentration on one other species, e.g., H_2 , must similarly be computed while the remaining species may be found from the element mass fractions given by the solution of Equation (15).

With this chemical system and with this selection of species to be determined by partial differential equations and by algebraic equations, it is possible to define the element mass fractions explicitly and to express the mass fraction species to be determined therefrom; thus

$$\tilde{Y}_1 \equiv Y_1 + (W_1/2W_3) Y_3 + Y_5 + (W_1/2W_7) Y_7 \quad (31)$$

$$\tilde{Y}_2 \equiv Y_2 + (W_2/W_3) Y_3 + Y_6 + (W_2/2W_7) Y_7 \quad (32)$$

$$\tilde{Y}_4 \equiv Y_4 \quad (33)$$

$$Y_1 = \tilde{Y}_1 - Y_5 - (W_1/2W_2)(\tilde{Y}_2 - Y_2 - Y_6) - (W_1/4W_7) Y_7 \quad (34)$$

$$Y_3 = W_3/W_2 (\tilde{Y}_2 - Y_2 - Y_6) - (W_3/2W_7) Y_7 \quad (35)$$

As mentioned previously it is possible for the mass fractions at a generic point to differ by many order of magnitude, thus making the solution of the algebraic Equations (31)-(35) highly inaccurate. For this reason the general description of the creation terms for all of the N species are given : (cf. eg., Reference 23, 24)

$$\dot{W}_i = W_i \sum_{j=1}^R (\nu_{ij}'' - \nu_{ij}') K_j \rho^{m_j} \prod_{l=1}^N (Y_l / W_l)^{\nu_{lj}'} \quad (36)$$

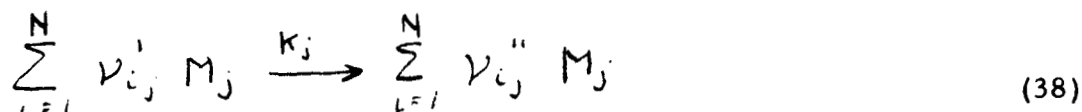
where

$$G_j = 1 - (\rho^{n_j} / K_{c,j}) \prod_{l=1}^N (Y_l / W_l)^{(\nu_{lj}'' - \nu_{lj}')} \quad (37)$$

$$m_j = \sum_{l=1}^N \nu_{lj}'$$

$$n_j = \sum_{l=1}^N (\nu_{lj}'' - \nu_{lj}')$$

where $K_{c,j}$ is the equilibrium constant based on molar concentrations for reaction j, and where ν_{ij}' and ν_{ij}'' are the stoichiometric coefficients of the reaction



Equations (30) and (36)-(38) permit the required $\dot{w}_{i,s}$ to be written as follows

$$\dot{W}_1 = W_1 \left\{ K_8 \rho^3 \frac{Y_5^2}{W_5^2 W} \left[1 - \frac{1}{\rho K_{c,8}} \frac{Y_1}{Y_5^2} \frac{W_5^2}{W_1} \right] - K_1 \frac{\rho^2}{W_1 W_6} Y_1 Y_6 \left[1 - \frac{1}{K_{c,1}} \frac{Y_5 Y_7}{Y_1 Y_6} \frac{W_1 W_6}{W_5 W_7} \right] \right\} \quad (39)$$

$$\dot{W}_2 = W_2 \left\{ -K_2 \frac{\rho^2}{W_2 W_5} Y_2 Y_5 \left[1 - \frac{1}{K_{c,2}} \frac{Y_6 Y_7}{Y_2 Y_5} \frac{W_2 W_5}{W_6 W_7} \right] - K_3 \frac{\rho^2}{W_2 W_7} Y_2 Y_7 \left[1 - \frac{1}{K_{c,3}} \frac{Y_3 Y_6}{Y_2 Y_7} \frac{W_2 W_7}{W_3 W_6} \right] + K_5 \frac{\rho^3}{W_6^2 W} Y_6^2 \left[1 - \frac{1}{\rho K_{c,5}} \frac{Y_2}{Y_6^2} \frac{W_6^2}{W_2} \right] \right\} \quad (40)$$

$$\dot{W}_3 = W_3 \left\{ \kappa_3 \frac{\rho^2}{W_2 W_7} Y_2 Y_7 \left[1 - \frac{1}{\kappa_{c,3}} \frac{Y_3 Y_6}{Y_2 Y_7} \frac{W_2 W_7}{W_3 W_6} \right] \right. \quad (41)$$

$$+ \kappa_4 \frac{\rho^2}{W_7^2} Y_7^2 \left[1 - \frac{1}{\kappa_{c,4}} \frac{Y_3 Y_5}{Y_7^2} \frac{W_7^2}{W_3 W_5} \right]$$

$$\left. + \kappa_6 \frac{\rho^3}{W_6 W_7 W} Y_6 Y_7 \left[1 - \frac{1}{\rho \kappa_{c,6}} \frac{Y_3}{Y_6 Y_7} \frac{W_6 W_7}{W_3} \right] \right\} \quad (42)$$

$$\dot{W}_4 = 0$$

$$\dot{W}_5 = W_5 \left\{ \kappa_1 \frac{\rho^2}{W_1 W_6} Y_1 Y_6 \left[1 - \frac{1}{\kappa_{c,1}} \frac{Y_5 Y_7}{Y_1 Y_6} \frac{W_1 W_6}{W_5 W_7} \right] \right. \quad (43)$$

$$- \kappa_2 \frac{\rho^2}{W_2 W_5} Y_2 Y_5 \left[1 - \frac{1}{\kappa_{c,2}} \frac{Y_6 Y_7}{Y_2 Y_5} \frac{W_2 W_5}{W_6 W_7} \right]$$

$$+ \kappa_4 \frac{\rho^2}{W_7^2} Y_7^2 \left[1 - \frac{1}{\kappa_{c,4}} \frac{Y_3 Y_5}{Y_7^2} \frac{W_7^2}{W_3 W_5} \right]$$

$$- \kappa_7 \frac{\rho^3}{W_5 W_6 W} Y_5 Y_6 \left[1 - \frac{1}{\rho \kappa_{c,7}} \frac{Y_7}{Y_5 Y_6} \frac{W_5 W_6}{W_7} \right]$$

$$+ 2 \kappa_8 \frac{\rho^3}{W_5^2 W} Y_5^2 \left[1 - \frac{1}{\rho \kappa_{c,8}} \frac{Y_1}{Y_5^2} \frac{W_5^2}{W_1} \right] \left. \right\}$$

$$\begin{aligned} \dot{w}_6 = W_6 \left\{ -\kappa_1 \frac{\rho^2}{w_1 w_6} Y_1 Y_6 \left[1 - \frac{1}{\kappa_{c,1}} \frac{Y_5 Y_7}{Y_1 Y_6} \frac{w_1 w_6}{w_5 w_7} \right] \right. \\ + \kappa_2 \frac{\rho^2}{w_2 w_5} Y_2 Y_5 \left[1 - \frac{1}{\kappa_{c,2}} \frac{Y_6 Y_7}{Y_2 Y_5} \frac{w_2 w_5}{w_6 w_7} \right] \\ + \kappa_3 \frac{\rho^2}{w_2 w_7} Y_2 Y_7 \left[1 - \frac{1}{\kappa_{c,3}} \frac{Y_3 Y_6}{Y_2 Y_7} \frac{w_2 w_7}{w_3 w_6} \right] \\ - 2 \kappa_5 \frac{\rho^3}{w_6^2 w} Y_6^2 \left[1 - \frac{1}{\rho \kappa_{c,5}} \frac{Y_2}{Y_6^2} \frac{w_6^2}{w_2} \right] \\ - \kappa_6 \frac{\rho^3}{w_6 w_7 w} Y_6 Y_7 \left[1 - \frac{1}{\rho \kappa_{c,6}} \frac{Y_3}{Y_6 Y_7} \frac{w_6 w_7}{w_3} \right] \\ \left. - \kappa_7 \frac{\rho^3}{w_5 w_6 w} Y_5 Y_6 \left[1 - \frac{1}{\rho \kappa_{c,7}} \frac{Y_2}{Y_5 Y_6} \frac{w_5 w_6}{w_7} \right] \right\} \end{aligned} \quad (44)$$

$$\begin{aligned} \dot{w}_7 = W_7 \left\{ \kappa_1 \frac{\rho^2}{w_1 w_6} Y_1 Y_6 \left[1 - \frac{1}{\kappa_{c,1}} \frac{Y_5 Y_7}{Y_1 Y_6} \frac{w_1 w_6}{w_5 w_7} \right] \right. \\ + \kappa_2 \frac{\rho^2}{w_2 w_5} Y_2 Y_5 \left[1 - \frac{1}{\kappa_{c,2}} \frac{Y_6 Y_7}{Y_2 Y_5} \frac{w_2 w_5}{w_6 w_7} \right] \\ - \kappa_3 \frac{\rho^2}{w_2 w_7} Y_2 Y_7 \left[1 - \frac{1}{\kappa_{c,3}} \frac{Y_3 Y_6}{Y_2 Y_7} \frac{w_2 w_7}{w_3 w_6} \right] \\ - 2 \kappa_4 \frac{\rho^2}{w_7^2} Y_7^2 \left[1 - \frac{1}{\kappa_{c,4}} \frac{Y_3 Y_5}{Y_7^2} \frac{w_7^2}{w_3 w_5} \right] \\ - \kappa_6 \frac{\rho^3}{w_6 w_7 w} Y_6 Y_7 \left[1 - \frac{1}{\rho \kappa_{c,6}} \frac{Y_3}{Y_6 Y_7} \frac{w_6 w_7}{w_3} \right] \\ \left. + \kappa_7 \frac{\rho^3}{w_5 w_6 w} Y_5 Y_6 \left[1 - \frac{1}{\rho \kappa_{c,7}} \frac{Y_2}{Y_5 Y_6} \frac{w_5 w_6}{w_7} \right] \right\} \end{aligned} \quad (45)$$

The equilibrium constants $K_{c,j}$ in these equations are available in tabular form, e.g., in Reference 24 but for computation it is convenient to represent them in functional form, namely

$$K_{c,j} \cong A_j T^{N_j} e^{B_j/T}$$

The constants A_j and B_j employed here with T in $^{\circ}\text{K}$ are as follows:

j	A_j	N_j	B_j $^{\circ}\text{K}$
1	12.1	0	8,150
2	2.31	0	1,540
3	0.23	0	-7930
4	10.4	0	-9490
5	1.85×10^4	-1	-54,000
6	9.66×10^4	-1	-62,200
7	8×10^3	-1	-52,500
8	9.67×10^4	-1	-60,600

where A_j is non-dimensional for $j = 1-4$ and is cc/gm for $j = 5-7$.

Several comments concerning the four Equations (39)-(42) may be in order. It will be noted that formally the creation terms given in general by Equation (36) can be written as

$$\dot{W}_c = W_c \sum_{j=1}^K (\nu_{c,j}'' - \nu_{c,j}') \tilde{\sigma}_j \quad (46)$$

where $\tilde{\sigma}_j$ is clearly defined by comparison between Equations (36) and (46). There are only K values of $\tilde{\sigma}_j$ to be computed. Also the form of Equation 39-45) readily admit application of the partial equilibrium treatment for boundary layer as

discussed in general form in Reference 23. This approximation should be valid for the hydrogen-air system at relatively high pressure (one atmosphere or more) and for high static temperature prior to heat release (1000°K or more). According to this idealization of the reaction $G_j \simeq 0$, $j = 1, 2, 3$, so that only one reaction equation, i.e., only one creation term must be considered explicitly*. However, the approximation $G_j \simeq 0$ does not imply that $\sigma_j = 0$; indeed $\tilde{\sigma}_j \sim k_j G_j$. Now the partial equilibrium approximation $G_j \simeq 0$ implies $K_j \rightarrow \infty$ and $\tilde{\sigma}_j$ is indeterminate, taking on whatever value is necessary to insure locally in the flow partial equilibrium. One technique for handling these indeterminacies is given in Reference 23. Finally, since the creation terms \dot{w}_i are non-dimensionalized with regard to $\mu_e / \rho_e^2 u_e^2$ it might be convenient to factor from the $\left\{ \right\}$ brackets a quotient k_0 / W_e where k_0 is a reference rate constant with units $(\text{mole/cc})^{-1} \text{sec}^{-1}$ and to insert in the same brackets ρ_e^{-2} ; this is suggested by the non-dimensionality of $(k_0 \mu_e / W_e u_e^2)$.

*The application of this approximation may be the subject of future research.

IV. CALCULATIONS:

Numerical solutions have been obtained for a number of cases of interest to the hydrogen dumping problem using an I. B. M. 7090 digital computer. It was decided to make use of all seven species conservation equations to avoid any algebraic difficulties. In addition, a curve fit of the velocity field in the following form was employed:

$$\begin{aligned} f'(\eta) &= .4694\eta - .02594\eta^3 + .00304\eta^4 & \eta \leq .426 \\ f'(\eta) &= 1.0 & \eta \geq .426 \end{aligned} \quad (47)$$

The procedure by which the external boundary conditions were applied along with a detailed development of the finite difference equations and the computational scheme can be found in Appendix II. Determination of the initial conditions is the subject of Appendix I.

Following the solutions of Equations (8) and (19) for the stagnation enthalpy ratio, $g = h/h_e$, and the seven species mass fractions, Y_i , respectively. Equations (24) and (26) are used to determine the static temperature T and the density ratio ρ_e/ρ respectively. This completes the determination of the thermodynamic field and allows solution of equations 3a and 4a thereby performing the transformation of the solution back to the physical plane. The parameter $\bar{C} = \bar{\rho} \mu / \rho_e \mu_e$, appearing in Equation (4a) is evaluated along the wall ($\eta = 0$) with the aid of Equations (28) and (29).

In addition, the heat transfer to the wall given by:

$$-\dot{q} = \pi \frac{\partial T}{\partial y} = \frac{1.8}{\sqrt{25}} \bar{C} \rho_e \mu_e H_e \left. \frac{\partial g}{\partial \eta} \right|_{\eta=0} \left(\frac{\text{BTU}}{\text{ft}^2 \cdot \text{sec}} \right) \quad (48)$$

and the displacement thickness:

$$\delta^* = \int_0^{\infty} \left(1 - \frac{\rho u}{\rho_e u_e}\right) dy = \frac{\mu_e \sqrt{25}}{\rho_e u_e} \int_0^{\infty} \left(\frac{\rho_e}{\rho} - \frac{u}{u_e}\right) d\eta \quad (49)$$

were evaluated. The method given in Reference (24) was used to obtain an estimate of the induced pressure forces acting on the plate. Finally, whenever possible, comparisons with the approximate collocation technique of Reference (27) were made.

The general conclusion from this study is that the finite difference program as developed here worked satisfactorily only when the chemical reactions were slow, i.e., when long ignition distances prevail. With that restriction, computation time for boundary layer distances over which the hydrogen mass fractions become negligible is throughout the boundary layer approximately 30-40 minutes. Thus a program of utility in connection with heterogeneous but non-reactive slot flows is available. However, when the reactions are fast enough to lead to significant chemical reaction, it was found that the streamwise step size had to be taken so small that computation was impractical. The difficulty has been studied and was found to be associated with the "stiffness" of the equations controlling the free radical generation, i.e., H, OH, and O. The concept of "stiffness" is discussed in Reference (28), however, the suggested technique of solution was found to yield poor numerical results for the systems under consideration. It was seen from the study that the speed of the reactions involving the above mentioned free radicals resulted in instability of the finite difference procedure for step sizes larger than a limiting step related to the inverse of the large reaction rate coefficients.

A solution to the impasse described above has been found which completely eliminates the difficulty.* This new procedure will be incorporated into the analysis at the earliest opportunity. It is anticipated that the boundary layer computation with energetic reaction will take no longer than those mentioned above for pure diffusion.

V. RESULTS AND CONCLUSIONS:

In Reference (15) a study was performed to determine the ignition delay times, (i.e., the interval of time between the initiation of chemical reaction and the noticeable release of heat) of hydrogen-air systems under various launch conditions. From this it appears that a trajectory point corresponding to an altitude of 45 km (150,000 ft.) and a Mach number of approximately 5, yields the minimum ignition delay time and hence represents conditions most favorable for the combustion and heat release of the slot injected hydrogen. These external conditions were therefore investigated. In addition, it was decided to investigate the effect of a change in the external conditions on the boundary layer flow due to an oblique shock wave induced in the vicinity of the slot.

The numerical cases considered were denoted as Cases I, II, and III. External flow conditions for Case I corresponded to a trajectory point at an altitude of 45 km and a Mach number 5. In cases II and III respectively, the constant external conditions considered corresponded to those present immediately downstream of a 45° and a 60° oblique shock with upstream conditions corresponding to Case I. In all cases

*A new technique has been found by Dr. Gino Moretti of GASL for handling the description of the chemical kinetics.

the wall or skin temperature was assumed to be 500°K . The temperature of the slot injected hydrogen was taken to be 75°K for Case I, and 100°K for Cases II and III. All the parameters of interest are recorded in Table I. Figures 1a-m and Figures 2a-m refer to Cases I and II respectively.

Under the idealization and assumptions underlying this study, the numerical finite-difference, finite rate-chemistry calculations indicate no combustion in the boundary layers of Case I and II within lengths of practical interest. In Case III, on the other hand, the program indicated the onset of reaction in a length of the order of 10 slot heights. Figures 1a, b, and 2a, b for Cases I and II respectively, show the initial mass fraction concentrations and stagnation enthalpy profiles obtained from the starting solutions outlined in Appendix I. Figures 1c-h and 2c-h show the mass fraction and static temperature profiles respectively at representative streamwise stations.

It is worthwhile to make some remarks at this point concerning the calculated static temperature profiles. Characteristic of hypersonic air boundary layers are high static temperatures within the boundary layer. It is, in fact, their high temperatures which might usually be expected to initiate the chemical reaction within the boundary layer. Examinations of Figures 1f-h show no such high static temperatures for an appreciable distance downstream of the slot.

This is attributed to the cooling effect of the cold, high heat capacity hydrogen which, in the laminar mixing model, persists in sufficient

quantities in the region of the wall for distances large in comparison to bodies of interest. Indeed one first begins to notice this temperature "pop" (Figure 1h) on the order of thousands of feet downstream of the injection point. (This conclusion may have to be modified by more careful consideration of the large normal gradients in density, specific heat and transport parameters as noted in Reference 29.) Hence, under the idealization of the flow presented here, at no place in the fields of the Case I and II boundary layers do static temperatures of the order of the hydrogen air ignition temperature appear and therefore no combustion is observed for those cases.

Figures 1_j and 2_j show the wall distribution of mass fractions. The dotted lines represent the solution of the approximate collocation technique given in Reference (30). As can be seen, the approximate solution appears to differ by a streamwise scale factor of approximately an order of magnitude. This is perhaps the type of accuracy to be expected from such an approximate analysis. Figures 1k, l and 2k, l show the displacement thicknesses and corresponding induced pressure distributions. The calculated displacement thicknesses were curve fitted and linearized supersonic flow theory was used to obtain the pressure distributions whereby:

$$C_p = \frac{2}{\gamma M_\infty^2} \frac{d\delta^*}{dx}$$

Smaller displacement thicknesses are given by the collocation solution since a more rapid diffusion is predicted by this approximate theory. Hence, at a given streamwise station the density will be

greater and displacement thickness smaller for the collocation solution than for the finite difference solution. Finally, the heat transfer to the plate is shown in Figures 1n and 2n. Here again, the more rapid diffusion of the cold hydrogen away from the wall, in the approximate solution accounts for higher predicted heat transfer rates.

VI. LIST OF SYMBOLS

a = slot height

$C_{pi}; \Delta_i$ = constants appearing in Equation 22

D_i = binary diffusion coefficient

$g = \frac{h_s}{h_{se}}$

h = static enthalpy

h_s = stagnation enthalpy

p = static pressure

s = transformed coordinate defined by Equation 4

T = static temperature

u = axial velocity

v = normal velocity

V_i = diffusion velocity of each species

W_i = molecular weight of species i

W = mean molecular weight of mixture $= \left(\sum_{i=1}^N \frac{Y_i}{W_i} \right)^{-1}$

w_i = creation term for species i due to K reaction

x = axial coordinate

y = normal coordinate

Y_i = mass fraction of species i

\tilde{Y}_i = mass fraction of element i

k = thermal conductivity

η = transformed coordinate defined by Equation 3

μ = viscosity

ρ = mass density

VII. References

1. Lees, L., "Convective Heat Transfer with Mass Addition and Chemical Reactions", Combustion and Propulsion, Third AGARD Colloquium, Palermo, Pergamon Press, New York, pp. 451-498, 1958.
2. Dennison, M. R., and Dooley, D. A., "Combustion in the Laminar Boundary Layer of Chemically Active Subliming Surfaces", J. Aeronautical Sciences, 25, 4, pp. 271-272, April, 1958.
3. Cohen, C. B., Bromberg, R., and Lipkis, R., "Boundary Layer with Chemical Reactions Due to Mass Addition", Jet Propulsion, 28, 10, pp. 659-668, October, 1958.
4. Eschenroeder, A. Q., "Combustion in the Boundary Layer of Porous Surfaces", J. Aeronautical Sciences 27, 12, pp. 901-906, December, 1960.
5. Dorance, W. A., "Viscous Hypersonic Flows", McGraw, Hill Book Company, Inc., 1962.
6. Libby, P. A., and Economos, C., "A Flame Zone Model of Chemical Reaction in a Laminar Boundary Layer with Application to the System of Hydrogen-Oxygen Mixtures" (To appear in the International Journal of Heat and Mass Transfer, also available as Report ARL 199, PIBAL 722, October, 1961).
7. Marble, F. E., and Adamson, T. C., Sr., "Ignition and Combustion in a Laminar Mixing Zone", Jet Propulsion, Volume 24, No. 2, pp. 85-94, April, 1954.
8. Dooley, D. A., "Ignition in the Laminar Boundary Layer of a Heated Plate", 1957, Heat Transfer and Fluid Mechanics Institute, pp. 321-342, Stanford University Press, California, 1957.
9. Chang, P., and Anderson, A. D., "Heat Transfer Around Blunt Bodies with Non-Equilibrium Boundary Layers, 1960, Heat Transfer and Fluid Mechanics Institute, Stanford University Press, 1960.
10. Vaglio-Laurin, R., and Bloom, M. H., "Chemical Effects in External Hypersonic Flows", Proceeding of the International Hypersonics Conference, August 16-18, 1961, M. I. T., Cambridge, Massachusetts.

11. Libby, P. A., Pergament, H., and Bloom, M. H., "A Theoretical Investigation of Hydrogen-Air Reactions", Part I, Behavior with Elaborate Chemistry, General Applied Science Laboratories TR No. 250, AFOSR-1378, August, 1961.
12. Ferri, A., Libby, P. A., and Zakkay, V., "Theoretical and Experimental Investigation of Supersonic Combustion" (To appear in the proceedings of the Third ICAS, Stockholm, September, 1962, also available in ARL Report No. 62-467, PIBAL No. 713, September, 1962.)
13. Duff, R. W., "Calculation of Reaction Profiles Behind Steady State Shock Lines," I, Application to Detonation Waves, Journal of Chemical Physics, Volume 28, p. 1193, 1958.
14. Schottl, G. L., "Kinetic Studies of Hydroxyl Radicals in Shock Waves", III The OH Concentration Maximum in the Hydrogen-Oxygen Reaction, Journal of Chemical Physics, Vol. 32, No. 2, pp. 710-716, March, 1960.
15. Libby, P. A., Pergament, H. S., and Taub, P., "Engineering Estimates of Flow Lengths Associated with the Combustion of Hydrogen-Air Mixtures During a Launch Trajectory", GASL TR No. 330, December, 1962.
16. Lees, L., "Laminar Heat Transfer over Blunt Nosed Bodies at Hypersonic Flight Speeds", Jet Propulsion 26, 259-269, 274, 1956.
17. Hayes, W. D., and Probstein, R. F., "Hypersonic Flow Theory", Academic Press, New York and London, 1959.
18. Libby, P. A., and Fox, H., "Some Perturbation Solutions in Laminar Boundary Layer Theory, Part II," The Energy Equation, PIBAL 752, October, 1963.
19. Libby, P. A., "Theoretical Analysis of Turbulent Mixing of Reactive Gases with Application to Supersonic Combustion of Hydrogen", ARS Journal Vol. 32, No. 3, pp. 388-396, March, 1962.
20. Libby, P. A., and Taub, P., "Analysis of Chemically Reacting Boundary Layers of Non-Uniform Composition with Application to Hydrogen Dumping," GASL TR 386.
21. Emanuel, G., and Vincent, W. G., "Method of Calculation of the One-Dimensional Non-Equilibrium Flow of a General Gas Mixture Through Hypersonic Nozzle", AEDC-TDR-L2-131, June, 1962.

22. Bromley, L. A., and Wilke, C. R., "Viscosity Behavior of Gases," Industrial and Engineering Chemistry, Vol. 43, July, 1951.
23. Libby, P. A., "Treatment of Partial Equilibrium Chemical Reacting Flows", JARS Vol. 32, No. 7, pp. 1090-1091, July, 1962.
24. Penner, S.S., "Chemistry Problems in Jet Propulsion", Pergamon Press, London, 1957.
25. Ting, L., "On the Mixing of Two Parallel Streams", Journal of Mathematics and Physics, Vol. 38, No. 3, October, 1959.
26. Toba, K., "Laminar Mixing of Two Parallel Streams in the Proximity of a Semi-Infinite Flat Plate", PIBAL #641, September, 1962.
27. Rosenbaum, H., "Induced Pressure Forces Due to Hydrogen Dumping", GASL TR-365, July, 1963.
28. Curtiss, C. F., and Hirschfelder, T. O., "Integration of Stiff Equations", Proc. of the National Academy of Science, Vol. 38, 1952.
29. Ferri, A., "Axially Symmetric Heterogeneous Mixing", PIBAL No. 787, September, 1963.
30. Taub, P.A., "Slot Injection of Reactive Gases in Laminar Flow with Application to Hydrogen Dumping", GASL TR 332, Jan., 1963.
31. Richtmyer, R. D., "Difference Methods for Initial-Value Problems", New York, Interscience Publisher, 1957.

APPENDIX I

DETERMINATION OF THE INITIAL CONDITIONS*

In order to provide in a rational way the initial conditions on the stagnation enthalpy, on the element mass fractions and on the species mass fractions so that the finite difference calculations can proceed, an analysis of the initial region of the flow, i.e., the region corresponding to $0 < x < x_i$ in Figure 3 is presented. In this special analysis the assumptions of the main analysis with respect to the flow and to the gas are applicable. In addition, it is assumed that both the external stream and the jet stream are supersonic and are at sufficiently low temperature so that no chemical reaction takes place in the length x_i .

The problem involved can be described physically in terms of Figure 3 and pertains to the determination of the actual orientation in the physical plane of the free mixing region. The indeterminacy of free mixing flows is well known; Ting (Reference 25) provided the means for removing this indeterminacy. Ting invokes the following considerations: because of the nature of the boundary layer formulation of the problem of free mixing, a boundary condition is lost and the solution for the velocity is indeterminate. However, if the second order pressures which are induced by the viscous flow are considered, and if it is required that at each streamwise station the induced pressure at $\pm \infty$ in the normal direction and in the boundary layer sense, must be equal, the indetermin-

*The authors are indebted to Dr. Lu Ting for helpful suggestions concerning the analysis presented here.

ancy is removed. Toba (Reference 26) applied these considerations to a flow similar to that treated here, but incompressible.

With this point of view established it is now possible to proceed with the analysis; it is necessary to consider the free mixing in such a manner that the normal coordinates are prescribed with respect to an arbitrarily selected streamline. Subsequently, the orientation of this streamline in the physical plane will be determined. In terms of the curvilinear coordinate system, s_1, y_1 with velocity components u_1 and v_1 , the flow equations to the boundary layer approximation are

$$\rho u_1 \frac{\partial u_1}{\partial x_1} + \rho v_1 \frac{\partial v_1}{\partial y_1} = \frac{\partial}{\partial y_1} \left(\mu \frac{\partial u_1}{\partial y_1} \right) \quad (I-1)$$

$$\frac{\partial(\rho u_1)}{\partial x_1} + \frac{\partial(\rho v_1)}{\partial y_1} = 0 \quad (I-2)$$

$$\rho u_1 \frac{\partial h_s}{\partial x_1} + \rho v_1 \frac{\partial h_s}{\partial y_1} = \frac{\partial}{\partial y_1} \left(\mu \frac{\partial h_s}{\partial y_1} \right) \quad (I-3)$$

$$\rho u_1 \frac{\partial Y_i}{\partial x_1} + \rho v_1 \frac{\partial Y_i}{\partial y_1} = \frac{\partial}{\partial y_1} \left(\mu \frac{\partial Y_i}{\partial y_1} \right) \quad (I-4)$$

where the same approximations relative to the Prandtl and Lewis numbers have been employed as in the main analysis and furthermore the flow is taken to be nonreactive.* The coordinates x_1 and y_1 are

*This assumption can be practically justified if the static temperatures T_e and T_i are less than T_i ; then no reaction will occur until oxygen and hydrogen mix in the portion of the boundary layer wherein viscous dissipation provides static temperatures in excess to T_i .

related to the physical coordinates by the equations (cf. Figure III)

$$\begin{aligned} x_1 &\approx x \\ y_1 &\approx y - z - a \end{aligned} \quad (I-5)$$

where it is assumed that $dz/dx \ll 1$ and where the line $z=z(x)$ is the streamline passing through the point $(0, a)$. Similarly the velocity components u_1 and v_1 are related to u and v by the equations

$$\begin{aligned} u_1 &\approx u \\ v_1 &\approx v - u \frac{dz}{dx} \end{aligned} \quad (I-6)$$

Consider a solution of Equations (I-1) and (I-2) in the usual fashion; introduce a streamfunction $\psi_1(x_1, y_1)$ so that

$$\begin{aligned} \rho u_1 &= \mu_e \frac{\partial \psi_1}{\partial y_1} \\ \rho v_1 &= -\mu_e \frac{\partial \psi_1}{\partial x_1} \end{aligned} \quad (I-7)$$

and introduce the transformations

$$\eta_1 = \frac{\rho_e u_e}{\mu_e \sqrt{2S_1}} \int_0^{y_1} \frac{\rho}{\rho_e} dy_1' \quad (I-8)$$

$$S_1 = \frac{\rho_e u_e}{\mu_e} \int_0^{x_1'} \bar{C}_1 dx_1' \quad (I-9)$$

where \bar{C}_1 is some suitably chosen representative value of the ratio $\rho u / \rho_e \mu_e$ for the mixing region. Continuing with the usual techniques for finding a similar solution assume

$$\psi_1 = \sqrt{2s_1} f_1(\eta_1) \quad (I-10)$$

Then Equation (I-1) becomes

$$f_1''' + f_1 f_1'' = 0 \quad (I-11)$$

where $()' \equiv d/d\eta_1$. The solution of (I-11) of interest in the present problem is

$$\begin{aligned} f_1' &= 1 \\ f_1 &= \eta_1 \end{aligned} \quad (I-12)$$

Note that the "third boundary condition" has in this case been taken to be $f_1(0) = 0$; thus, $\eta_1 = 0$ along the line $y = z(x) + a$. Also with that

$$\psi_1 = \psi - \frac{\rho_s u_s a}{\mu_s} \quad (I-13)$$

With the solution for the velocity field obtained in terms of η_1 the solution for the energy distribution can be obtained; transformation of Equation (I-3) to the s_1, η_1 variables followed by the assumption that $g_1 \equiv g_1(\eta_1)$ leads to

$$g_1'' + \eta_1 g_1' = 0 \quad (I-14)$$

which is subject to the conditions

$$g_1(\infty) = 1, \quad g_1(-\infty) = h_{s_1} / h_{s_e} \equiv \lambda_h \quad (I-15)$$

The solution is easily found to be

$$g = \left(\frac{1+\lambda_h}{2} \right) + \left(\frac{1-\lambda_h}{2} \right) \sqrt{\frac{2}{\pi}} \int_0^{\eta_1} e^{-x_1'^2} dx_1' \quad (I-16)$$

A similar analysis applies to the species conservation equation, namely to Equation (I-4); indeed, the equation for $Y_i = Y_i(\eta_1)$ is

$$Y_i'' + \eta_1 Y_i' = 0 \quad (I-17)$$

i.e., closely analogous to Equation (I-14). However, the boundary conditions are different; they are

$$\begin{aligned} Y_i(\infty) &= Y_{i,e} \\ Y_i(-\infty) &= Y_{i,j} \end{aligned} \quad (I-18)$$

The solution is

$$Y_i = \left(\frac{Y_{i,e} + Y_{i,j}}{2} \right) + \left(\frac{Y_{i,e} - Y_{i,j}}{2} \right) \sqrt{\frac{2}{\pi}} \int_0^{\eta_1} e^{-x_1'^2} dx_1' \quad (I-19)$$

The Equations (I-16) and (I-19) provide the distributions of energy and species concentration in terms of η_1 and therefore in terms of x_1 and y_1 . Indeed since $x_1 \simeq x$, it can be considered that the distributions in terms of x and y_1 are known.

There remains the determination of $z = z(x)$; to do so requires computations of the velocities v at $y = \pm\infty$. Consider first the velocities v_1 at $y_1 = \pm\infty$; in general, from the definition of ψ_1 .

(I-20)

$$\rho_1 v_1 = - \frac{\mu_e}{\sqrt{2s_1}} \left[2s_1 \frac{\partial \eta_1}{\partial x_1} f_1' + \frac{\rho_e u_e \bar{c}_1 f_1}{\mu_e} \right]$$

Now

$$\frac{\partial \eta_1}{\partial x_1} = - \frac{\eta_1}{2s_1} \left(\frac{\rho_e u_e \bar{c}_1}{\mu_e} \right) + \frac{\rho_e^2 u_e^2}{\mu_e^2 \sqrt{2s_1}} \int_0^{\eta_1} \frac{1}{\rho_e} \frac{\partial \rho}{\partial x_1} dy_1 \quad (I-21)$$

At $\eta_1 = \pm \infty$ the second term in the right hand side of Equation (I-21) becomes zero

so that

$$\rho v_1 \Big|_{\eta_1 = \pm \infty} = 0$$

This result implies that the induced pressure which arises from isovelocity free

mixing and which at $y_1 = \pm \infty$ would be equal to $u_e (\rho v_1) \Big|_{y_1 = \infty}$ is zero; thus

for $0 < x < x_0$, Equation (I-6) can be satisfied by $v_1 = v = dz/dx = 0$ implying $z = 0$

and the line in the free mixing solutions corresponding to $\psi_1 = \eta_1 = 0$ lies along the line in the physical plane corresponding to $y = a$.

To determine the orientation of the free mixing downstream of x_0 , it will be assumed that the velocities induced on the free mixing region from the boundary layer may be considered to be effective on the line $y = a$. It will be convenient for the further discussion to refer to Figure IV which shows the distribution of induced normal velocity computed along the line $y = a$. These distributions must be considered: That due to the boundary layer, and (that) due to the free mixing tilted with respect to the line $y = a$ and corresponding to $y_1 = \pm \infty$.

Now the induced velocity at $y = \infty$ due to the boundary layer is expressed as (cf. the analogous treatment of v_1 in Equations (I-20) and (I-21))

$$\rho_j V_\infty = \frac{\rho_e u_e \bar{C}_1 \eta}{\sqrt{2s}} \quad (I-22)$$

where n is a constant associated with the asymptotic behavior of f , namely as

$$\eta \rightarrow \infty, f \rightarrow \eta - n^* \dots$$

The velocities from the free mixing and due to the tilting dz/dx are equal at

$\eta_1 = \pm \infty$ and, since $v_1 \Big|_{y_1 \pm \infty} = 0$, are equal to $u_e dz/dx$. Thus if linearized supersonic theory is applied, the pressure induced on the lower surface of the line $y = a$ is

$$\frac{p^- - p_{\infty,j}}{\frac{1}{2} \rho_j u_j^2} = \frac{2}{\sqrt{M_j^2 - 1}} \left[\frac{\rho_e u_e \bar{C}_1 \eta}{\rho_j u_j \sqrt{2(s-s_0)}} - \frac{d\eta}{dx} \right] \quad (I-23)$$

where $s_0 = \left(\frac{\rho_e u_e}{\mu_e} \int_0^{x_0} \bar{C}_1 dx' \right)$; the pressure induced on the upper side of the line due to the free mixing again according to linearized supersonic theory is

$$\frac{p^+ - p_{\infty,e}}{\frac{1}{2} \rho_e u_e^2} = \frac{2}{\sqrt{M_e^2 - 1}} \frac{d\eta}{dx} \quad (I-24)$$

Now require that $p^+ = p^-$ and let $p_{\infty,e} = p_{\infty,j} = p_\infty$; then Equations (I-23) and I-24 yield for $u_j = u_e$, an equation for dz/dx ; namely

$$\frac{d\eta}{ds} = \frac{\mu_e \bar{C}_1 \eta}{\rho_j u_e \sqrt{2s}} \left[\frac{\rho_e \sqrt{M_j^2 - 1}}{\rho_j \sqrt{M_e^2 - 1}} + 1 \right]^{-1} = \frac{\alpha \bar{C}}{\sqrt{2s}} \quad (I-25)$$

where $\xi \equiv x - s_0$. The solution subject to the initial condition $z = 0$ at $\xi = 0$ is

*The value of n for the Blasius function is 1.378.

$$z = \alpha \int_0^{\xi} \frac{\bar{C}_1 d\xi'}{\sqrt{2\xi'}} \quad (\text{I-26})$$

or if \bar{C}_1 is taken to be constant for the regions $0 < x < x_2$, (cf. Figure III) i.e., $\bar{C}_1 = \bar{C}_1^*$, then

$$z = \alpha \bar{C}_1 \sqrt{2\xi} \quad (\text{I-27})$$

The free mixing solutions with the distortions associated with $z = z(\xi)$ from either Equations (I-26) or equations (I-27) is applied until the edge of the stagnation enthalpies and concentration distributions associated with free mixing approach the corresponding edges of the boundary layer. At the streamwise station at which this occurs, numerical integration by finite difference methods can be initiated. The determination of the length x_0 is complicated by the fact that the locations in the physical plane must be determined. Define by a value η_e the edge of the boundary layer, i.e., where $f' \approx 0.995$, e.g., and a lower edge of the free mixing by $\eta_{1,e}$. Note that $\eta_{1,e} < 0$. Finally define x_0 as the streamwise station at which the edges in operation are separated by $\Delta > 0$; thus

$$z + a \Big|_{x=x_0} = (y_e + \Delta + |y_{1,m}|) \quad (\text{I-29})$$

Consider the computation of each terms on the right hand side of Equation (I-29); clearly from the inverse of the transformation given by Equation (3)

$$y_e = \frac{\mu_e \sqrt{2\xi_0}}{\rho_e u_e} \int_0^{\eta_e} \frac{\rho_e}{\rho} d\eta' \quad (\text{I-30})$$

Similarly, from Equation (I-8) with $s_1 \approx s = s_0$

$$|y_{1,m}| = \left| \frac{\mu_e \sqrt{2s_0}}{\rho_e u_e} \int_0^{\eta_{1e}} \frac{\rho_e}{\rho} d\eta' \right| \quad (\text{I-31})$$

The solutions for the boundary layer and for the free mixing permit the integrals to be evaluated in terms of η and η_1 . Thus substitution of Equations (I-26) or I-27), and Equations (I-30) and I-31) with (I-29) permit s_0 to be obtained, where Δ is taken $\ll 1$

Then the solutions for the boundary layer and the free mixing in terms of η and η_1 , respectively, can be employed at $s = s_0$ to determine $h_{s,i}(\eta)$, $\tilde{Y}_{i,i}(\eta)$, and $Y_{i,i}(\eta)$ as required in the numerical integration.

APPENDIX II

DETAILS OF THE FINITE DIFFERENCE COMPUTATION

The eight partial differential equations to be solved by an implicit finite difference technique will be repeated here for convenience.

Let $z_i = Y_{i,i} - Y_{i,e}$ then,

$$\frac{\partial^2 z_i}{\partial \eta^2} + f \frac{\partial z_i}{\partial \eta} - 2s f' \frac{\partial z_i}{\partial s} + \frac{2s}{\tau} \frac{\rho_e}{\rho} \dot{\omega}_i \frac{\mu_e}{\rho_e^2 u_e^2} = 0 \quad (\text{II-1})$$

with the boundary conditions

$$\begin{aligned} \frac{\partial z_i(s, 0)}{\partial \eta} &= 0 \\ z_i(s, \infty) &= 0 \end{aligned}$$

and initial conditions

$$z_i(s, \eta) = z_{i,i}(\eta)$$

The energy equation is

$$\frac{\partial^2 g}{\partial \eta^2} + f \frac{\partial g}{\partial \eta} - 2s f' \frac{\partial g}{\partial s} = 0 \quad (\text{II-2})$$

with the boundary conditions

$$\begin{aligned} g(s, 0) &= h_{se} \left\{ \sum_{i=1}^2 Y_i C_{pi} (T - T_r) + \sum_{i=1}^2 Y_i \Delta_i \right\}_{\eta=0} \\ g(s, \infty) &= 1 \end{aligned}$$

with $T = T_w$ at $\eta = 0$

and with initial conditions

$$g(s, \eta) = g_i(\eta)$$

Referring to Figure V Equations (II-1) may be differenced to yield,
(Reference 31).

$$\alpha z_{j, \kappa+1} + \beta z_{j, \kappa} + \gamma z_{j, \kappa-1} = 2S_j F_{j-1, \kappa} \quad (\text{II-3})$$

where

$$\alpha = \left[\frac{1}{(\Delta\eta)^2} + \frac{f_{\kappa}}{2\Delta\eta} \right]$$

$$\beta = - \left[\frac{2}{(\Delta\eta)^2} + \frac{2S_j f'_{\kappa}}{\Delta S} \right]$$

$$\gamma = \left[\frac{1}{(\Delta\eta)^2} - \frac{f'_{\kappa}}{2\Delta\eta} \right] ; \quad F_{j-1, \kappa} = - \left[(w_i)_{j-1, \kappa} + \frac{f'_h(z)_{j-1, \kappa}}{\Delta S} \right]$$

The boundary condition

$$\frac{\partial z_i(s, 0)}{\partial \eta} = 0$$

implies $(z_i)_{1, j} = (z_i)_{-1, j}$

The boundary condition

$$z_i(s, \infty) = 0$$

implies

$$\frac{\partial z_i(s, \infty)}{\partial \eta} = 0$$

In order to apply this boundary condition numerically it is assumed that

at some

$$\eta = \bar{\eta} ; \quad \frac{\partial z_i(s, \bar{\eta})}{\partial \eta} = 0$$

The equations are then solved for all z_i and a test is performed to determine if:

$$z_i(s, \bar{\eta}) \leq \epsilon$$

where ϵ is some small number.

If the test fails a new value of $\bar{\eta} = \bar{\eta}_0 + \Delta\eta$ is chosen and the procedure is repeated until,

$$z_i(S, \bar{\eta}) \leq \epsilon$$

It should be noted that for each mesh point added on the j^{th} strip one must also be added on the $(j-1)^{\text{th}}$ strip. This, however, presents no difficulties since it can be assumed $z_i \sim 0$ for all $\eta > \bar{\eta}$. Hence the solution of the seven partial differential equations II-1 reduces to the solution of the $n+1$ linear algebraic equations given below in matrix form.

$$\begin{vmatrix} a_{11} & a_{12} & & & \\ & a_{21} & a_{22} & a_{23} & \\ & & & & \\ & & & & \\ & & & & \\ & & & & \\ & & & & a_{n+1,n} & a_{n+1,n+1} \end{vmatrix} \cdot \begin{vmatrix} z_{j,0} \\ z_{j,1} \\ \\ \\ z_{j,n} \end{vmatrix} = \begin{vmatrix} F_{j-1,0} \\ \\ \\ F_{j-1,n} \end{vmatrix} \quad (\text{III-3})$$

where

$$\left. \begin{aligned} a_{l,l+1} &= \alpha \\ a_{l,l} &= \beta \\ a_{l,l-1} &= \gamma \end{aligned} \right\} 1 \leq l \leq n$$

$$a_{11} = \beta$$

$$a_{12} = \alpha + \gamma$$

$$a_{n+1,n} = \alpha + \gamma$$

$$a_{n+1,n+1} = \beta$$

The general tridiagonal matrix

$$A = \begin{vmatrix} a_{11} & a_{12} & & \\ a_{21} & a_{22} & a_{23} & \\ & & & \\ & & a_{n-1,n-2} & a_{n-1,n-1} & a_{n-1,n} \\ & & & a_{n,n-1} & a_{n,n} \end{vmatrix}$$

can be decomposed into the product of a lower bidiagonal matrix **B** and an upper bidiagonal modified triangular matrix **C** which will significantly facilitate the solution of the system of linear equations $AX = F$.

This decomposition is accomplished in the following manner:

$$\begin{aligned} \alpha_i &= a_{ii} & i=1 \\ \gamma_{i-1} &= a_{i-1,i} / \alpha_{i-1} \\ \alpha_i &= a_{ii} - a_{i,i-1} \gamma_{i-1} \end{aligned} \quad \left. \vphantom{\begin{aligned} \alpha_i &= a_{ii} \\ \gamma_{i-1} &= a_{i-1,i} / \alpha_{i-1} \\ \alpha_i &= a_{ii} - a_{i,i-1} \gamma_{i-1} \end{aligned}} \right\} i > 1$$

let

$$B = \begin{vmatrix} \alpha_1 & & & \\ a_{21} & \alpha_2 & & \\ & & & \\ & & a_{n,n-1} & \alpha_n \end{vmatrix} \quad C = \begin{vmatrix} 1 & \gamma_1 & & \\ & 1 & \gamma_2 & \\ & & & \\ & & & \gamma_{n-1} & 1 \end{vmatrix}$$

Now the matrix equation: $AX = F$ is equivalent to $BCX = F$ and can be considered as $BY = F$ and solved for Y as follows:

$$\begin{aligned} Y_i &= F_i / \alpha_i & i=1 \\ Y_i &= \frac{F_i - a_{i,i-1} Y_{i-1}}{\alpha_i} & i=2, \dots, n \end{aligned}$$

Finally $CX = Y$ is solved for X :

$$\begin{aligned} X_n &= Y_n & i=n \\ X_{n-1} &= Y_{n-1} - \gamma_{n-1} X_n & i=n-1, \dots, 1 \end{aligned}$$

This completes the solution of the eight partial differential equations. While the implicit finite difference scheme is unconditionally stable for all Δs , $\Delta \eta$ particular attention must be paid to the coefficient

$$\gamma = \frac{1}{(\Delta \eta)^2} - \frac{f_{\eta}}{2\Delta \eta}$$

In the limiting case of $\Delta \eta$ approaching zero it is clear that γ is a positive number at all finite regions (s, η) of the field. However, for a finite value of the step size $\Delta \eta$, and for sufficiently large values of $\bar{\eta}$, it is seen that γ can become zero or negative due to the unbounded increase of f with η . Such behavior of γ corresponds to a large truncation error in the finite difference representation of the differential equations.

In order to obtain the proper asymptotic behavior for $\eta \rightarrow \bar{\eta}$ it was necessary to require

$$\left(\frac{1}{(\Delta \eta)^2} - \frac{f_{\eta}}{\Delta \eta} \right) > 0$$

A study of the difference equation with constant values of f_k was carried out. Closed form solutions of the difference equation for various values of $\Delta \eta$ were obtained and compared with the limiting form for $\Delta \eta \rightarrow 0$. It was found as a result of some numerical experimentation that a suitable criterion for $\Delta \eta$ was

$$\Delta \eta < \frac{1}{2f_{\eta}}$$

The implicit finite difference scheme places no requirements of the ratio of step sizes in the normal and streamwise directions. Accuracy

is then the only criterion for the step size in the s direction. The program includes an automatic procedure for determining the step size needed for a desired degree of accuracy. This is accomplished by computing the variables Z_i at step sizes of (Δs) and $(2 \Delta s)$. The quantity ϵ , where

$$\epsilon = \left| \frac{(Z_i)_{at (2\Delta s)} - (Z_i)_{at 2 (\Delta s)}}{(Z_i)_{at 2 (\Delta s)}} \right|$$

is computed at each $(2 \Delta s)$ and at every other Δs . Then if

$$.01 < \epsilon \leq 0.1$$

the step size Δs is retained. If

$$\epsilon \leq .01$$

the step size $(2\Delta s)$ is chosen. If

$$\epsilon > 0.1$$

the step size $\frac{\Delta s}{2}$ is chosen. The procedure is then repeated, automatically choosing the proper step size as the calculation proceeds.

TABLE I

A- General Parameters

$a = \text{slot height} = 1''$

$C_{p1} = .26403 \text{ cal/gm } ^\circ\text{k}$

$C_{p2} = .3654 \quad ''$

$C_{p3} = .56361 \quad ''$

$C_{p4} = .28382 \quad ''$

$C_{p5} = .3121 \quad ''$

$C_{p6} = .4968 \quad ''$

$C_{p7} = .43765 \quad ''$

$W_1 = 32$

$W_2 = 2$

$W_3 = 18$

$W_4 = 28$

$W_5 = 16$

$W_6 = 1$

$W_7 = 17$

$\Delta_1 = 185.23 \text{ cal/gm } ^\circ\text{k}$

$\Delta_2 = 2687.9$

$\Delta_3 = 2831.3$

$\Delta_4 = 200.05$

$\Delta_5 = 3938.1$

$\Delta_6 = 55,873.0$

$\Delta_7 = 911.78$

$T_r = 1040^\circ\text{k}$

$T_w = 500^\circ\text{k}$

TABLE II

Displacement thickness curve fits.

$$\delta^* = a_0 + a_1 x + a_2 x^2 + a_3 x^3$$

CASE I

	$x < 600$	$x \geq 600$
a_0	.33308	.74069
a_1	2.1195×10^{-3}	$.24660 \times 10^{-3}$
a_2	-3.3059×10^{-6}	$-.01020 \times 10^{-6}$
a_3	2.01164×10^{-9}	0

CASE II

	$x \leq 1800$	$x \geq 1800$
a_0	.075336	.257502
a_1	4.11022×10^{-4}	$.471604 \times 10^{-4}$
a_2	-26.378×10^{-8}	$-.21956 \times 10^{-8}$
a_3	70.306×10^{-12}	0

Table I (continued)

B-Case I

$$M_e = 5.3$$

$$u_c = 5780 \text{ ft./sec.}$$

$$\rho_e = 1.2388 \times .5 \text{ lb./ft.}^3$$

$$P_e = .00157 \text{ atm.}$$

$$T_e = 275.8 \text{ }^\circ\text{K}$$

$$\mu_e = 1.1654 \times .5^5 \text{ lb./sec.}^2\text{ft.}$$

$$T_j = 75^\circ\text{K}$$

C-Case II

$$M_e = 2$$

$$u_e = 4189 \text{ ft./sec.}$$

$$T_e = 1011.91 \text{ }^\circ\text{K}$$

$$P_e = .0255 \text{ atm.}$$

$$\rho_e = 5.4829 \times .5^4 \text{ lb./ft.}^3$$

$$T_j = 100 \text{ }^\circ\text{K}$$

D. Case III

$$M_e = 1.254$$

$$u_e = 3068.7 \text{ ft./sec.}$$

$$T_e = 1388.5 \text{ }^\circ\text{K}$$

$$P_e = .03833 \text{ atm.}$$

$$\rho_e = 6.0072 \times 10^{-4} \text{ lb./ft.}^3$$

$$\mu_e = 3.384 \times 10^{-5} \text{ lb./ft.}^2 \text{ sec.}$$

$$T_j = 100^\circ\text{K}$$

$$S_i = 1.7817 \times 10^4$$

Figure 1a

Initial Mass Fraction Distributions

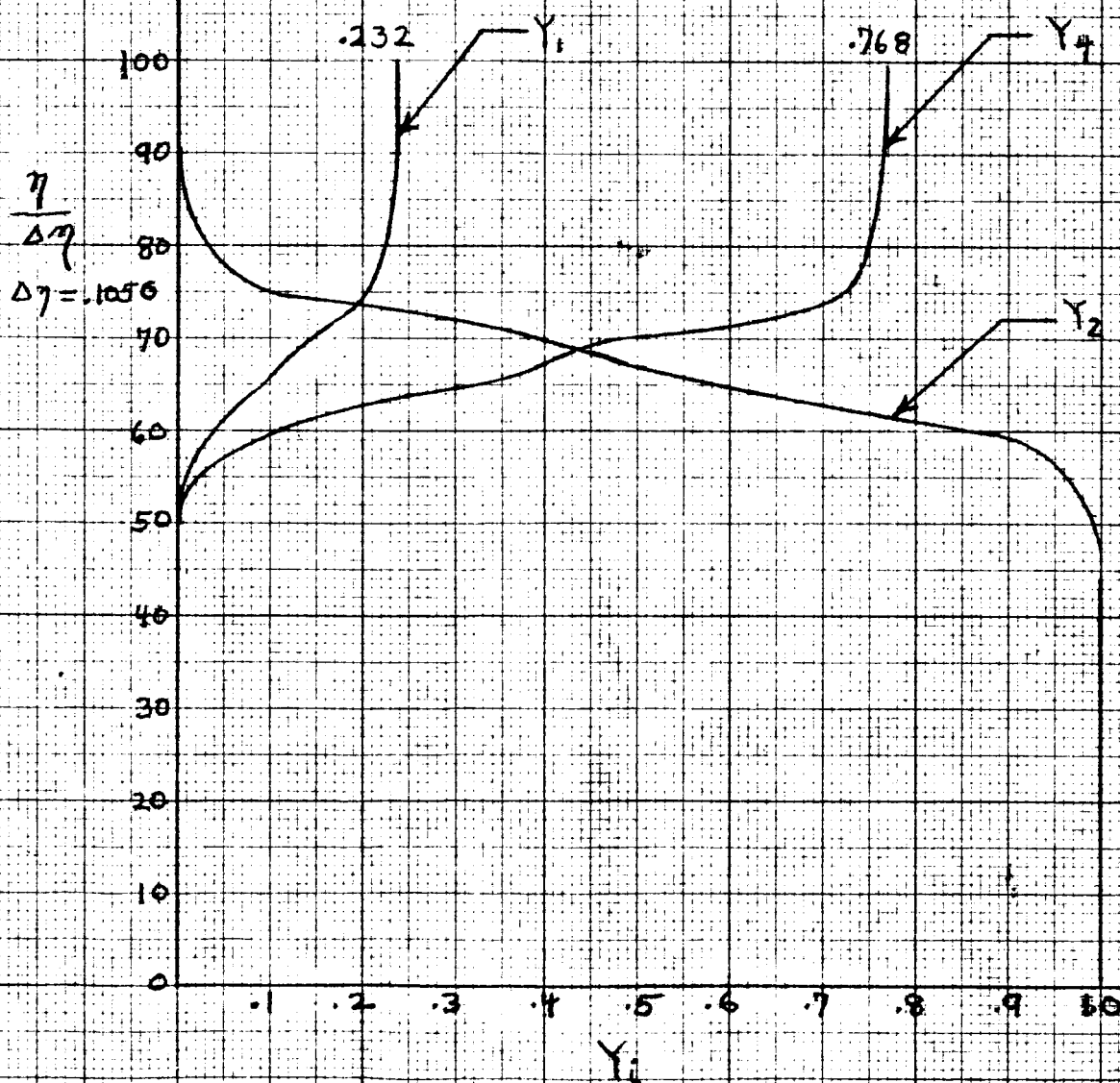


Figure 1b

Initial Stagnation Enthalpy Profiles

$$S_i = 1.28 \times 10^4$$

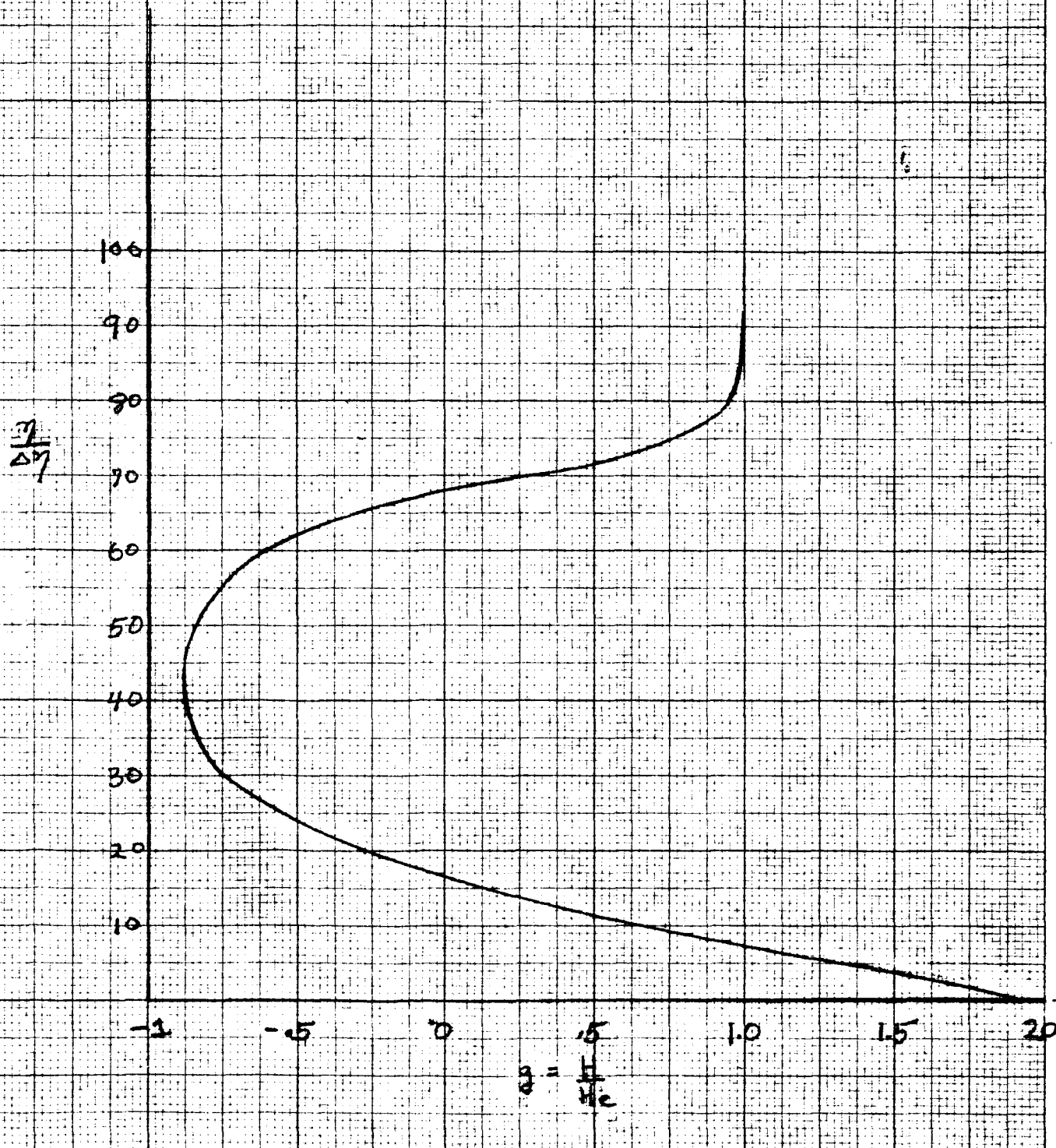


Figure 1c

Mass Fraction Distribution

$X = 90 \text{ ft}$

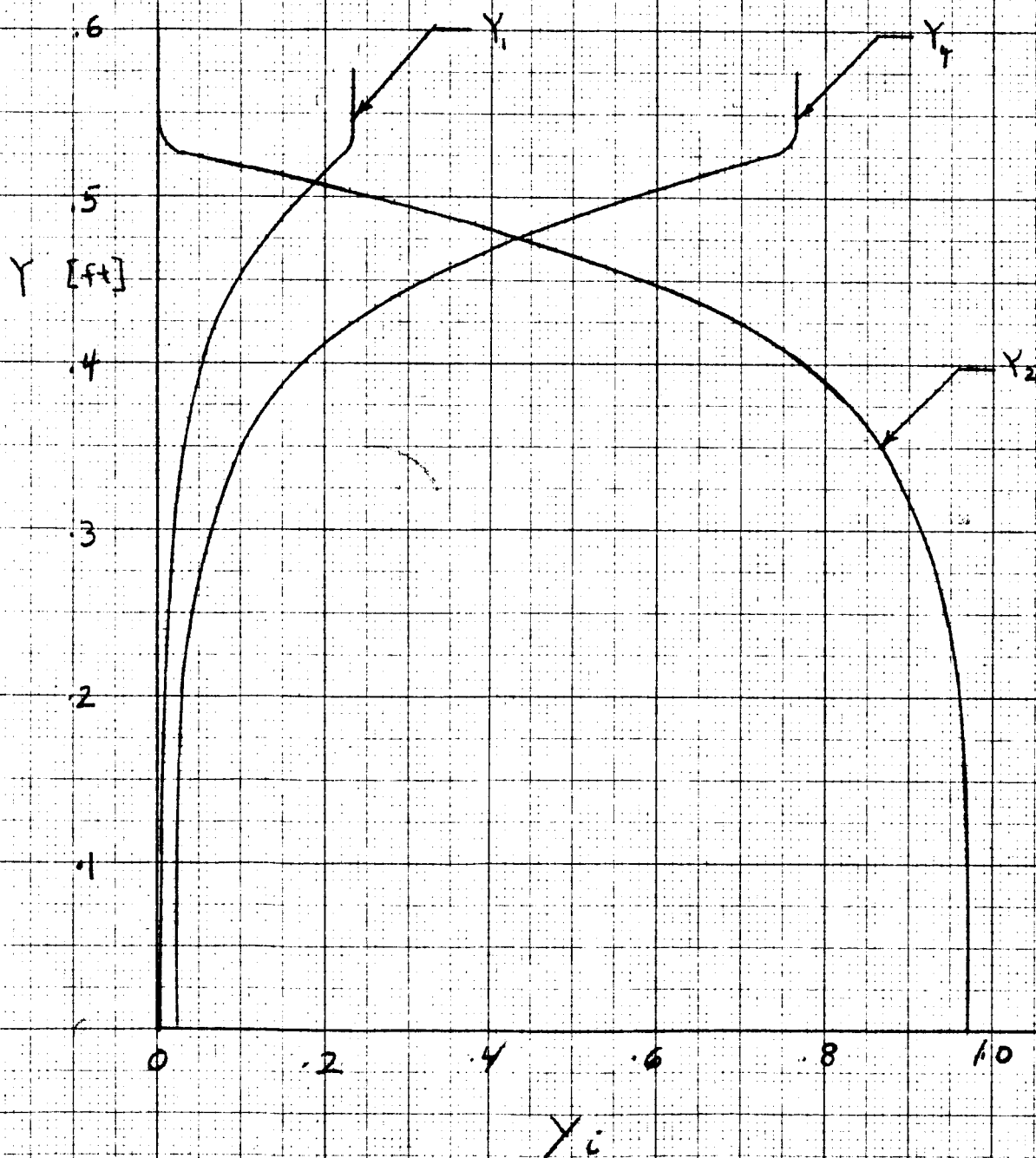
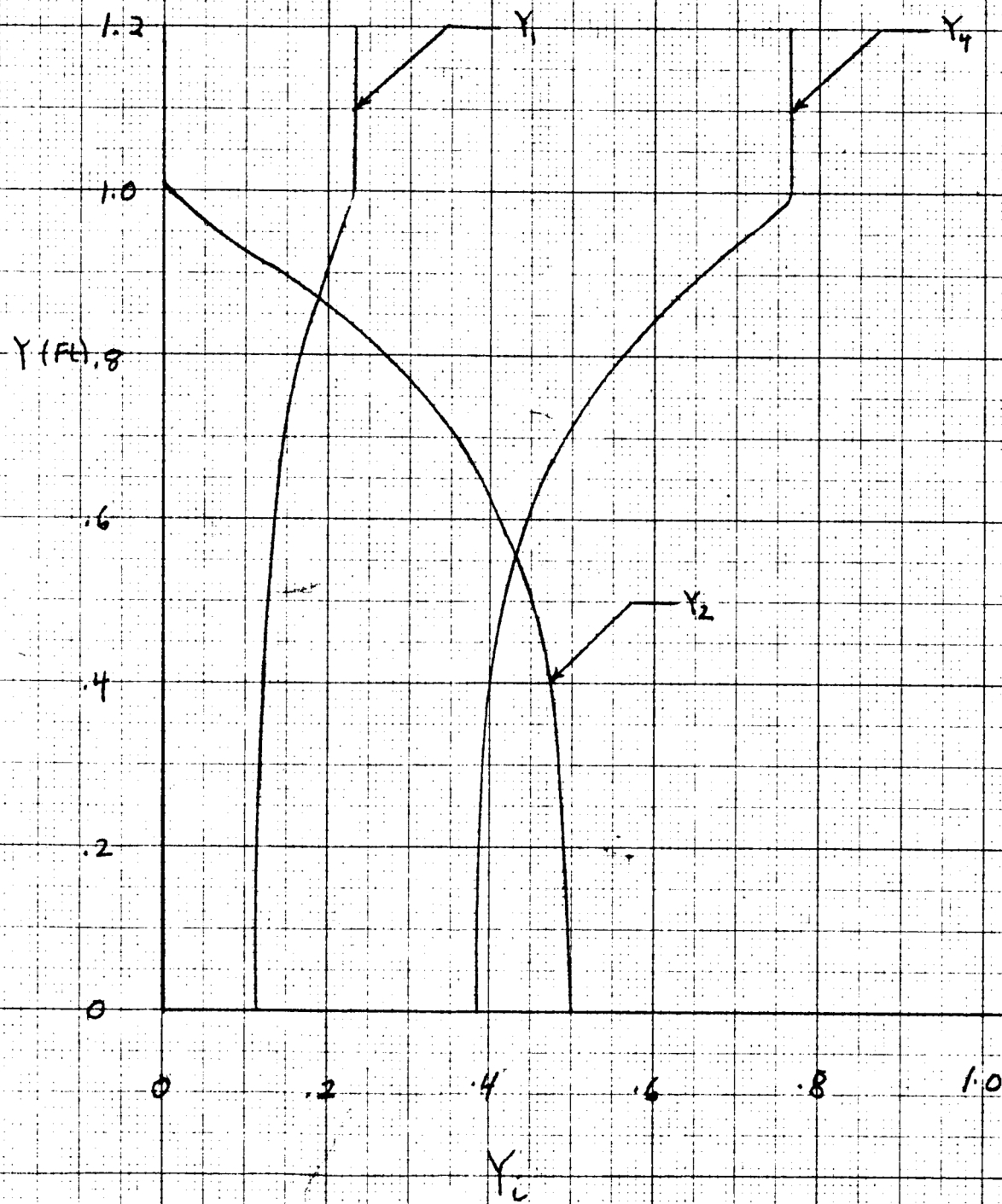


Figure 1d

$X = 741 \text{ ft}$ Mass Fraction Distribution



$X = 5,200 \text{ ft}$

Figure 1b

Mass Fraction Distribution

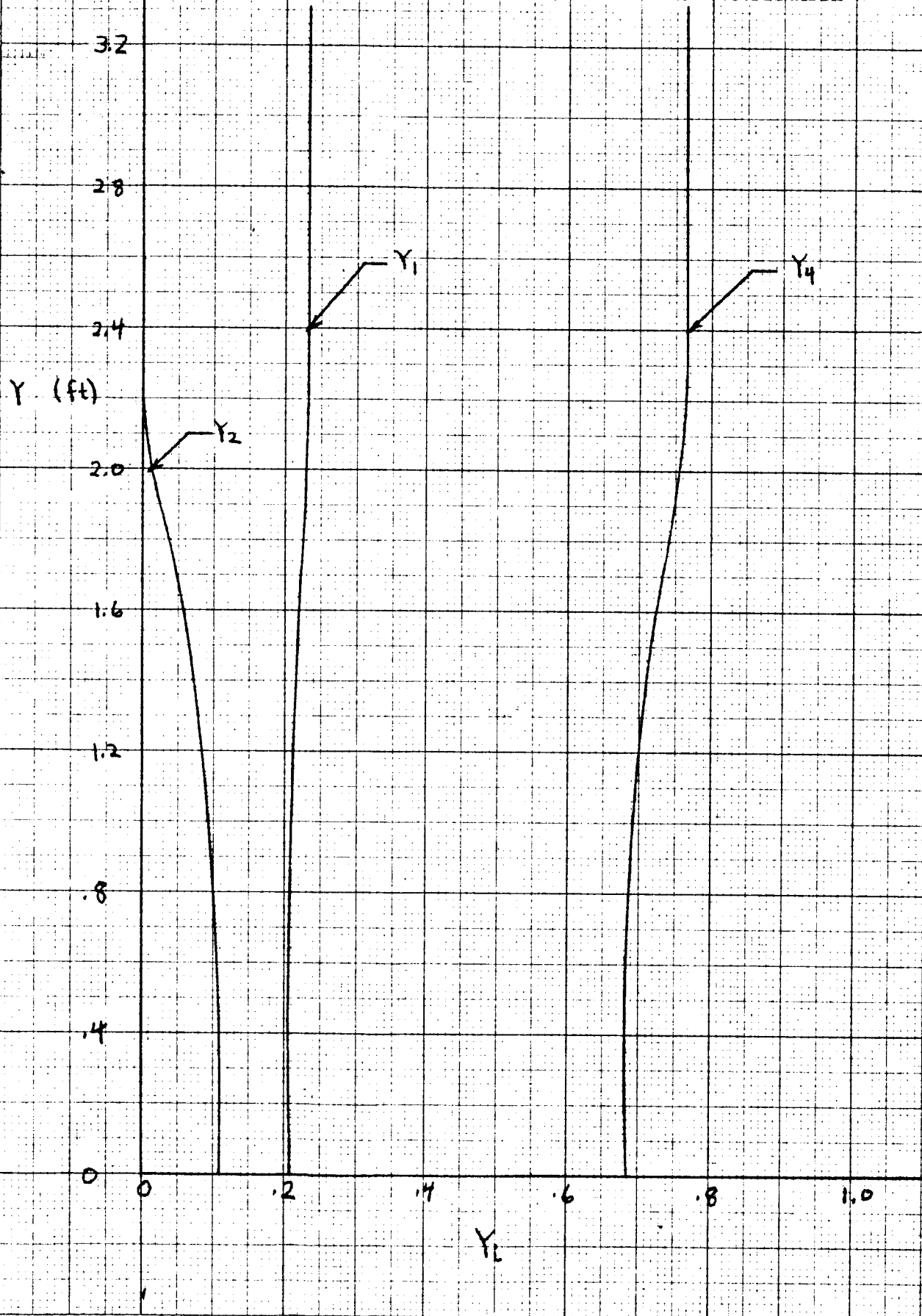


Figure 11

Static Temperature Distribution

$X = 90$ ft

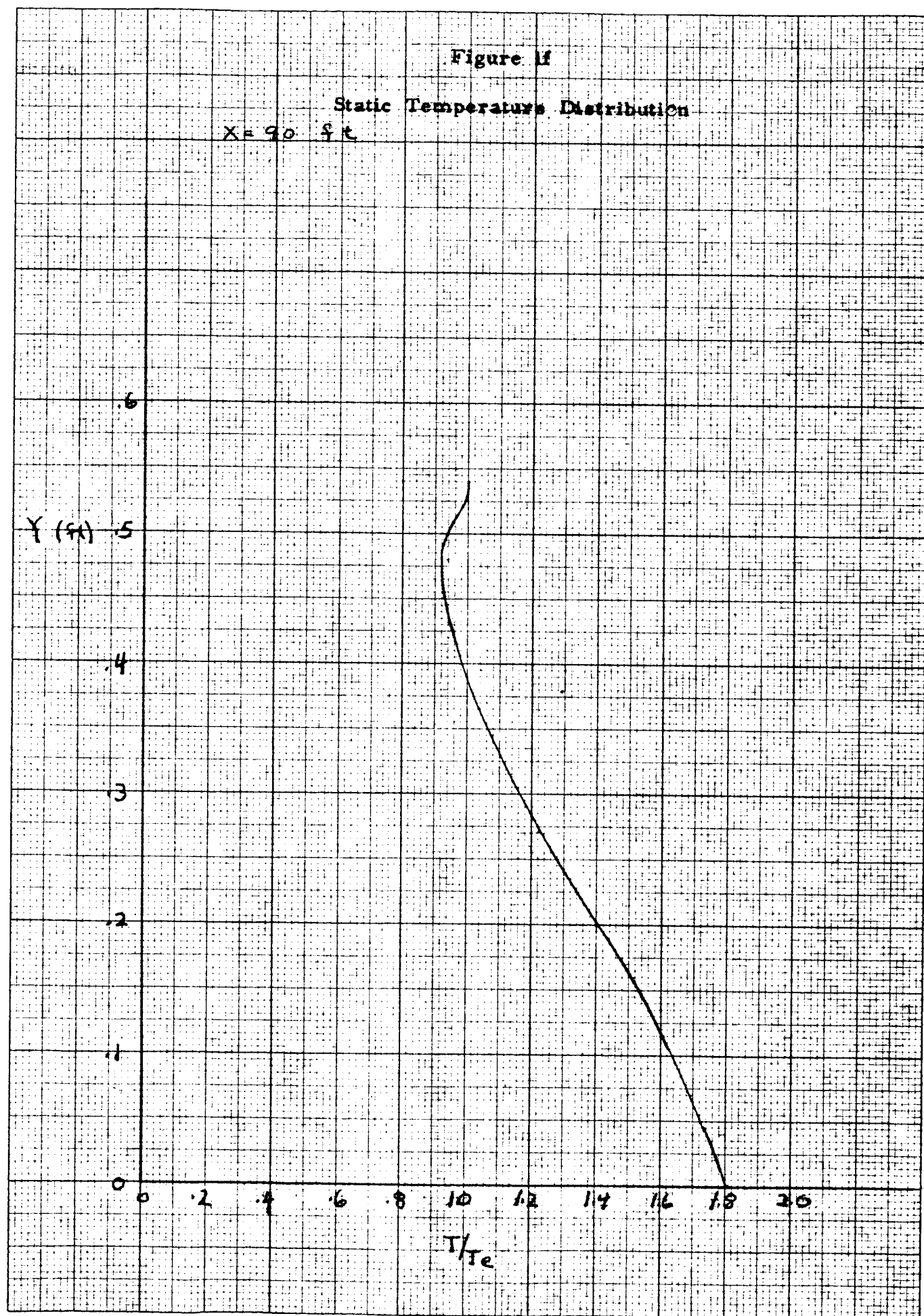


Figure 1g

Static Temperature Distribution

$X = 741 \text{ ft}$

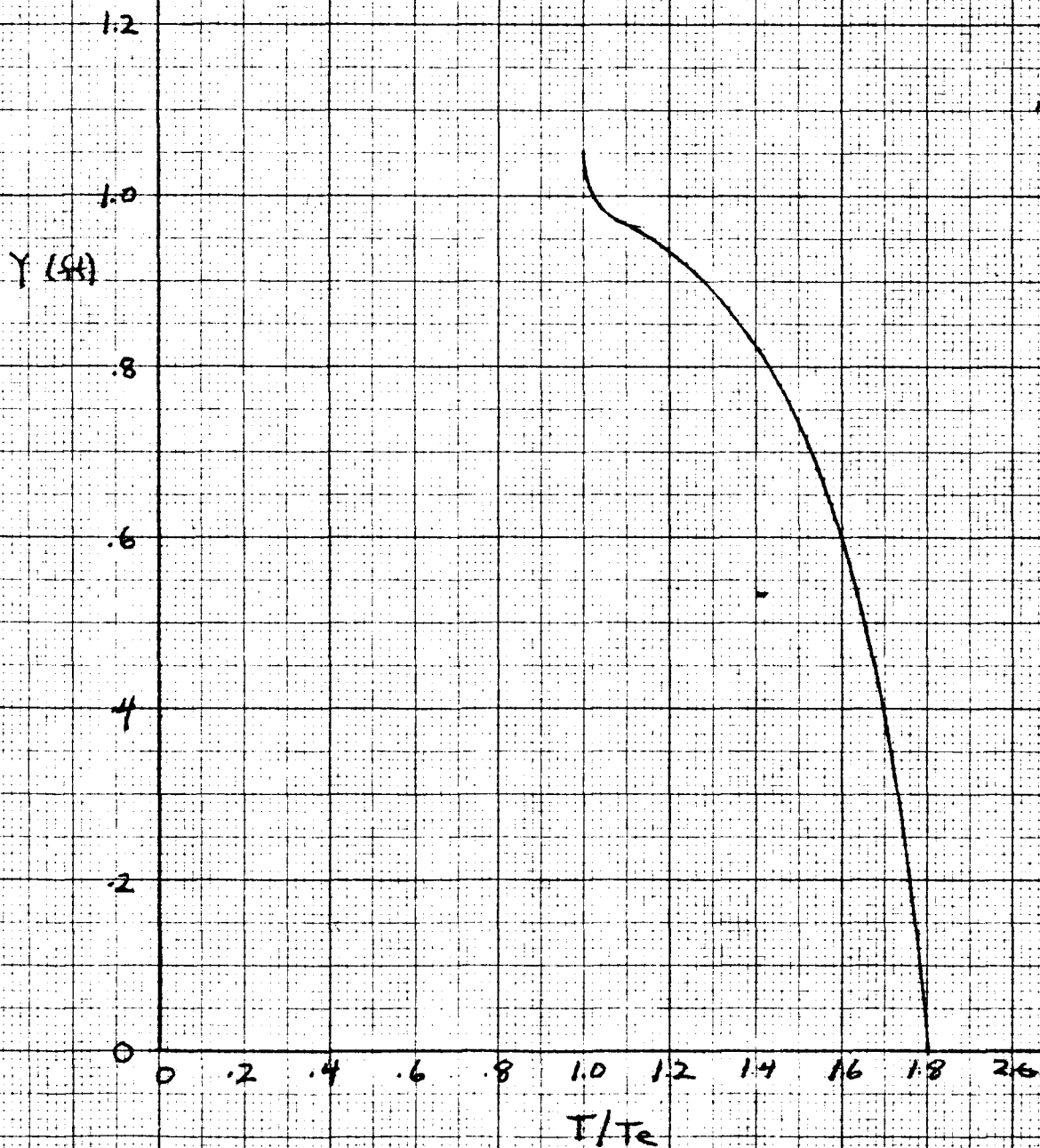
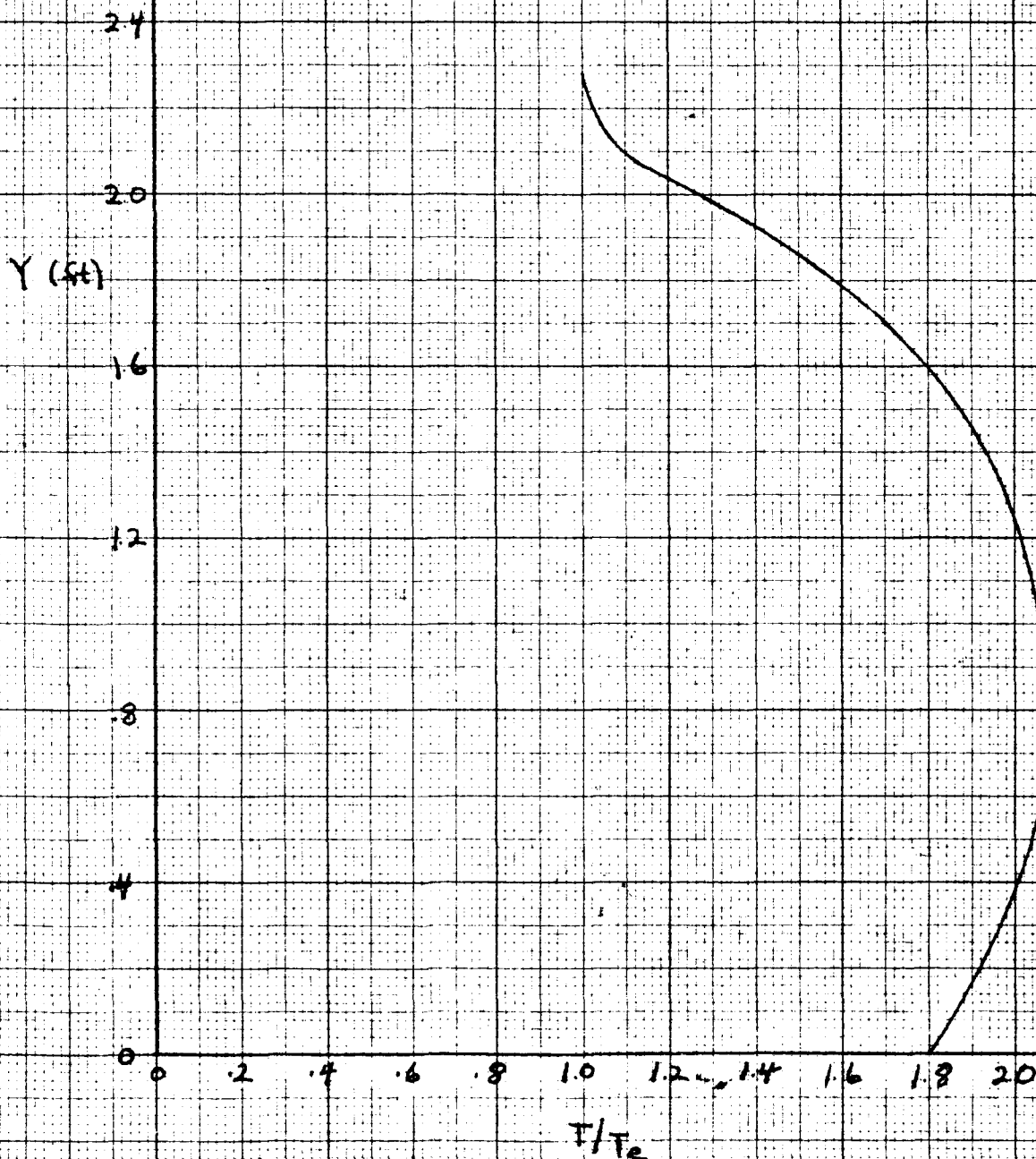


Figure 1h

Static Temperature Distribution

X = 5200 ft



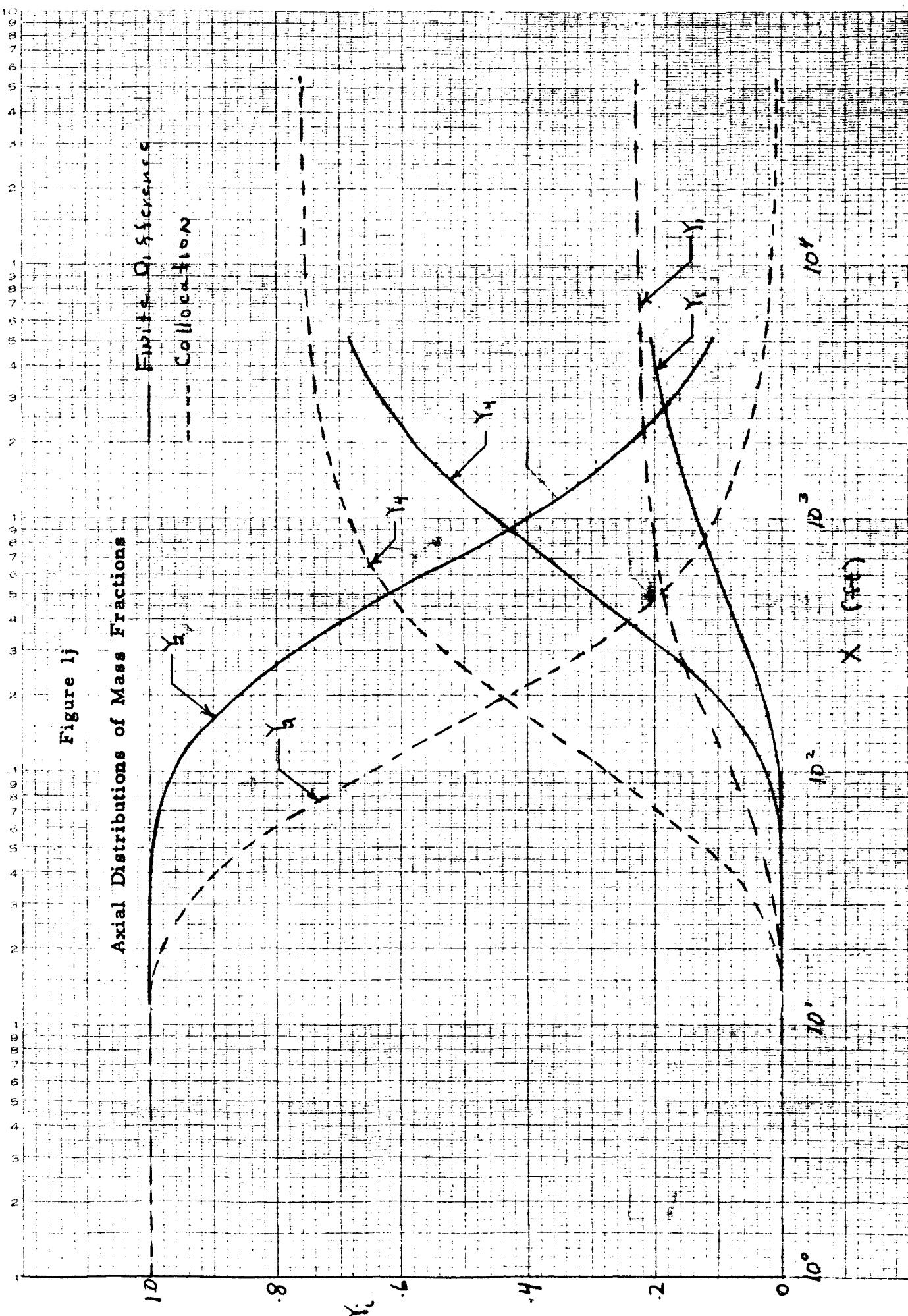


Figure 1j

Axial Distributions of Mass Fractions

Finite Differences

Collocation

10^4

10^3

10^2

10^1

10^0

X (ft)

Y_1

Y_2

Y_1

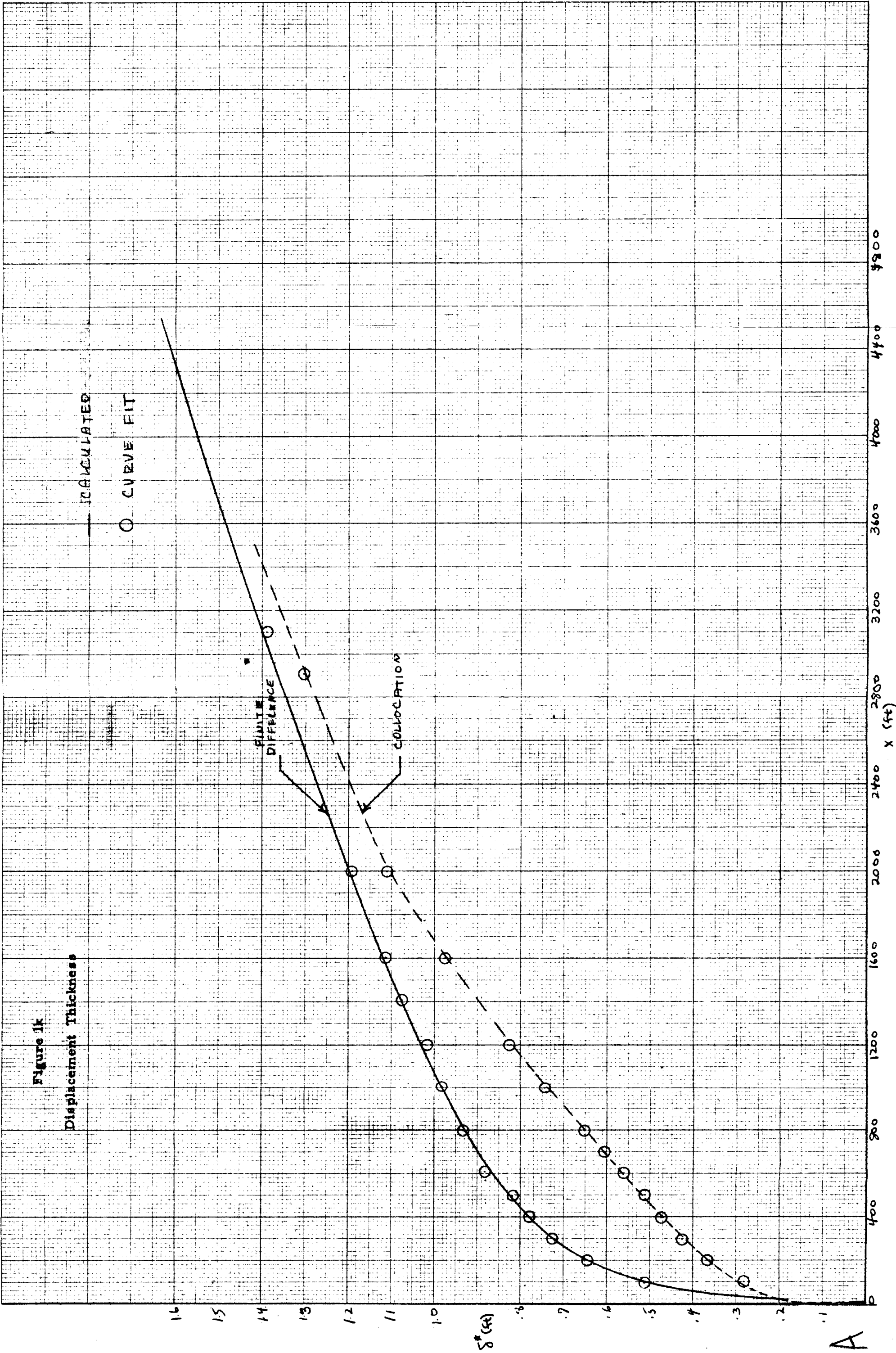
Y_2

Y_3

Y_4

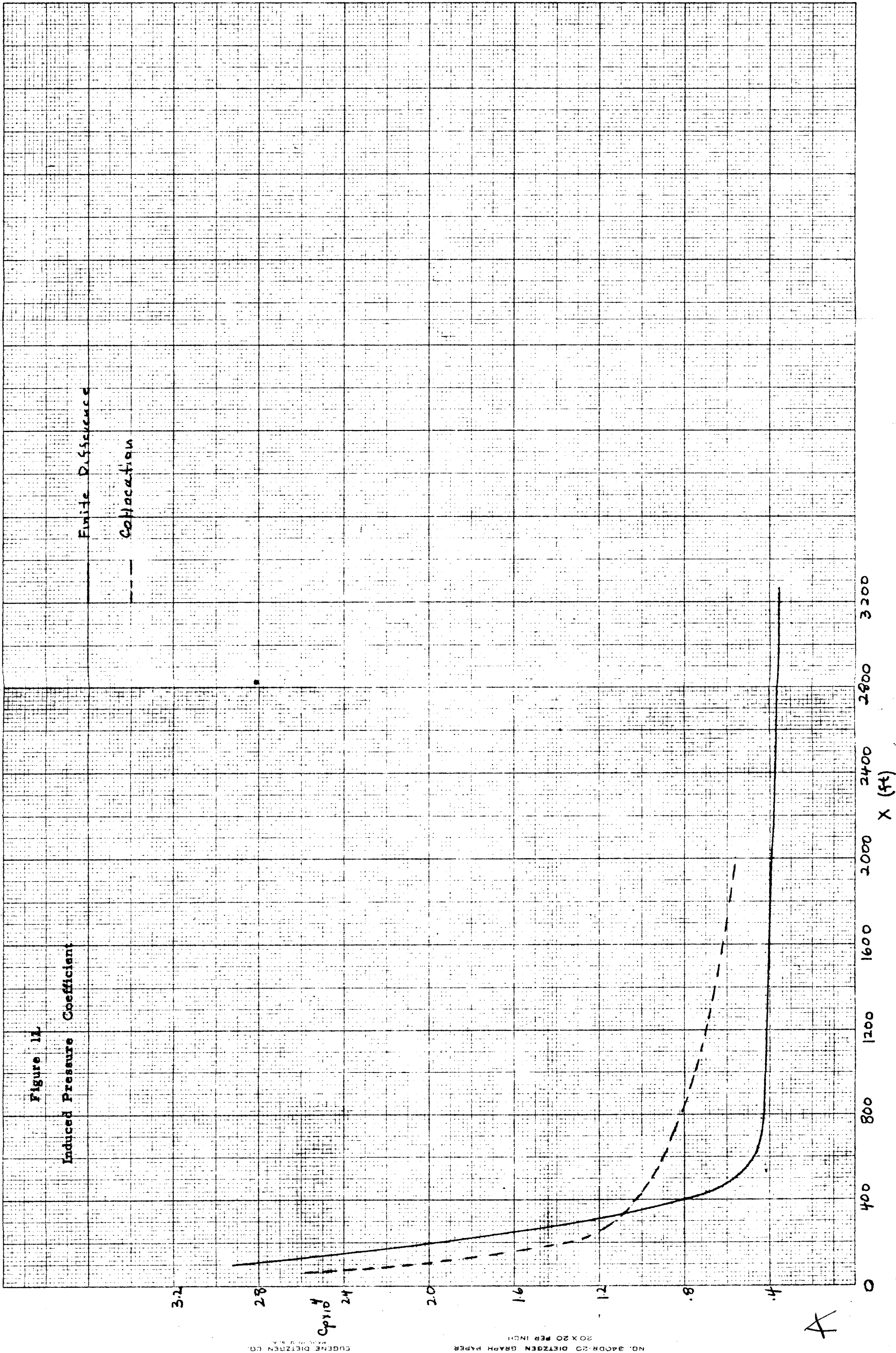
Y_1

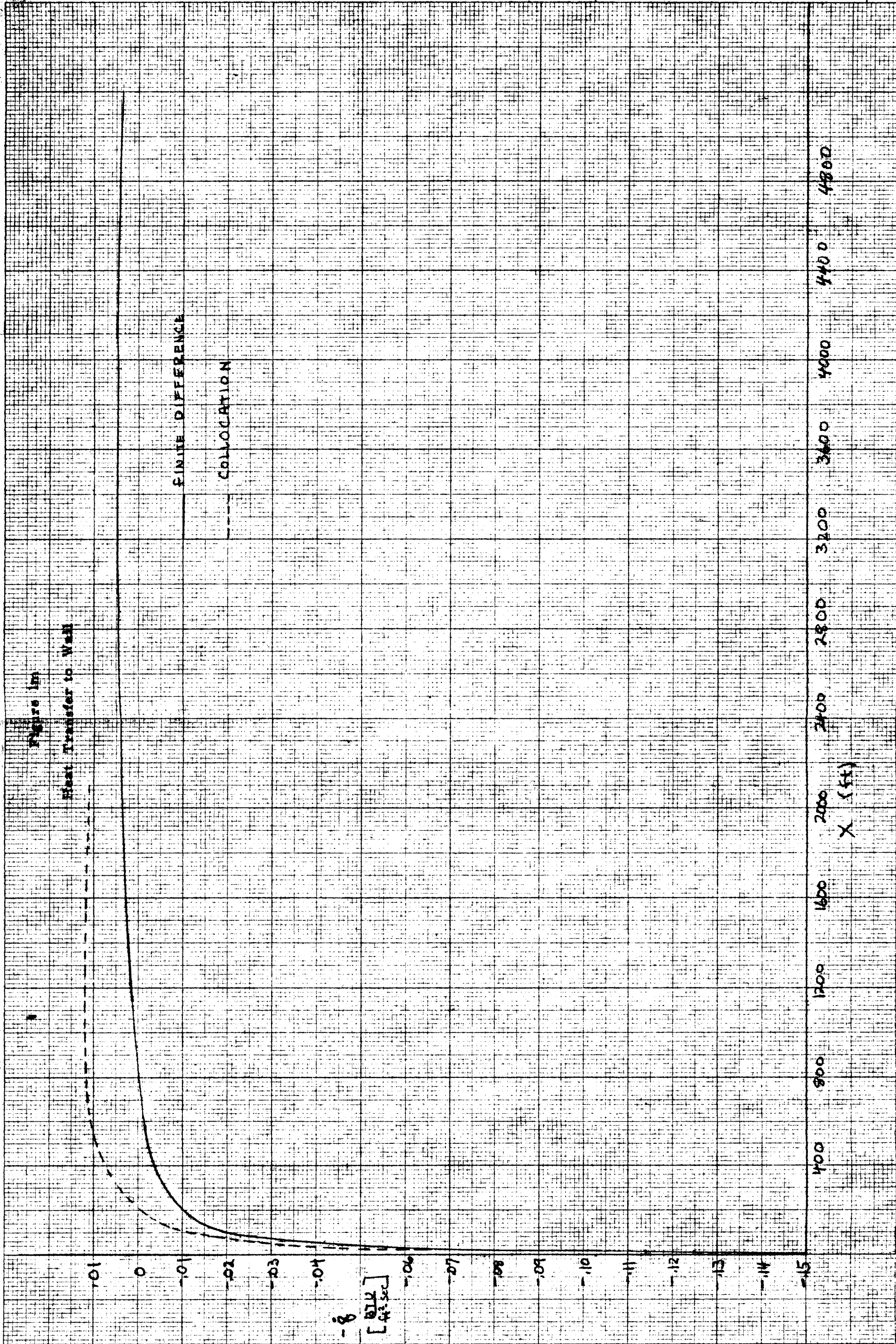
Y_2



A

B





$$S_0 = 9.72 \times 10^6$$

Figure 2a

Initial Mass Fraction Distributions

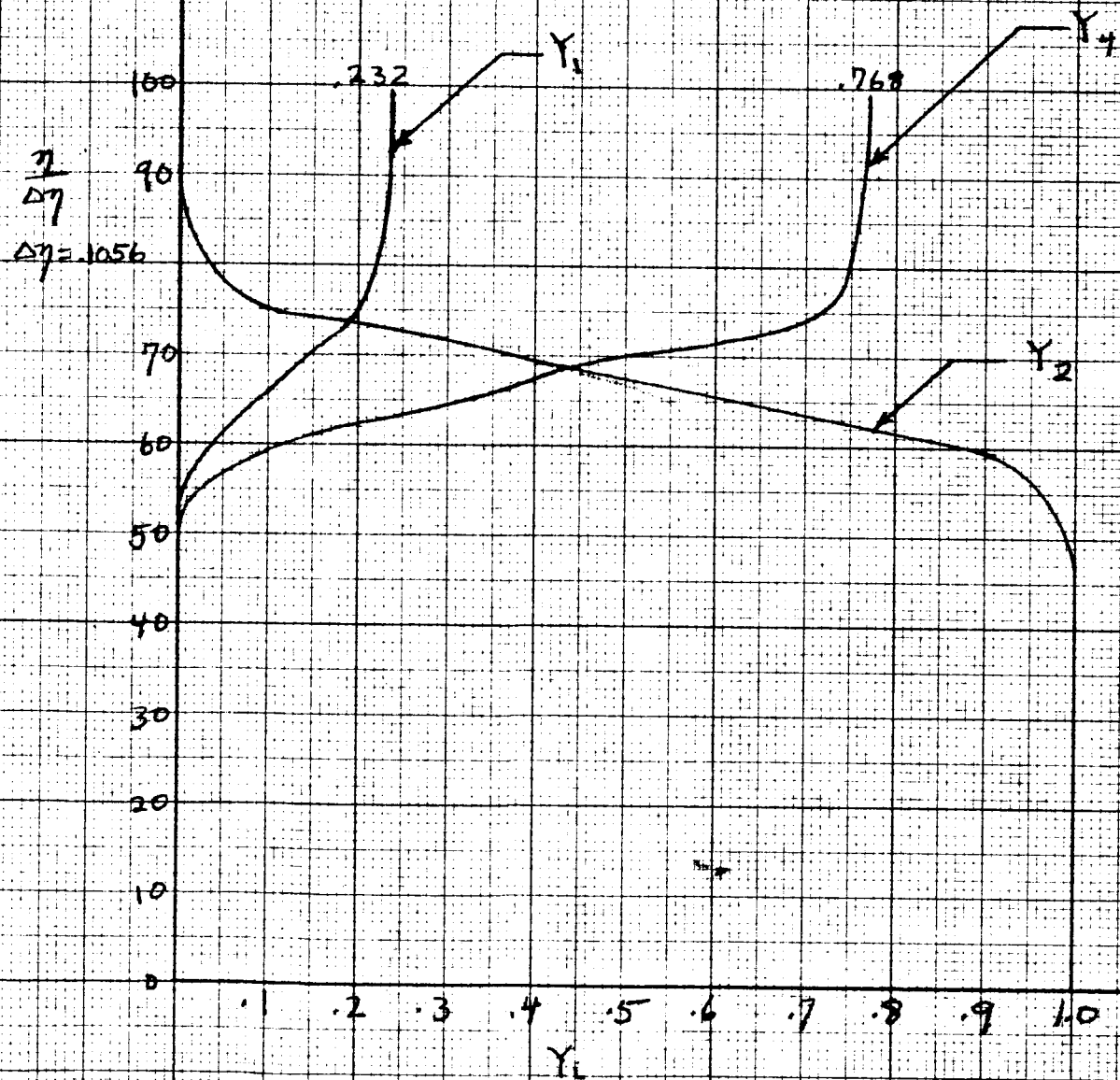


Figure 2b

Initial Stagnation Enthalpy Profiles

$$SL = 9.72 \times 10^5$$

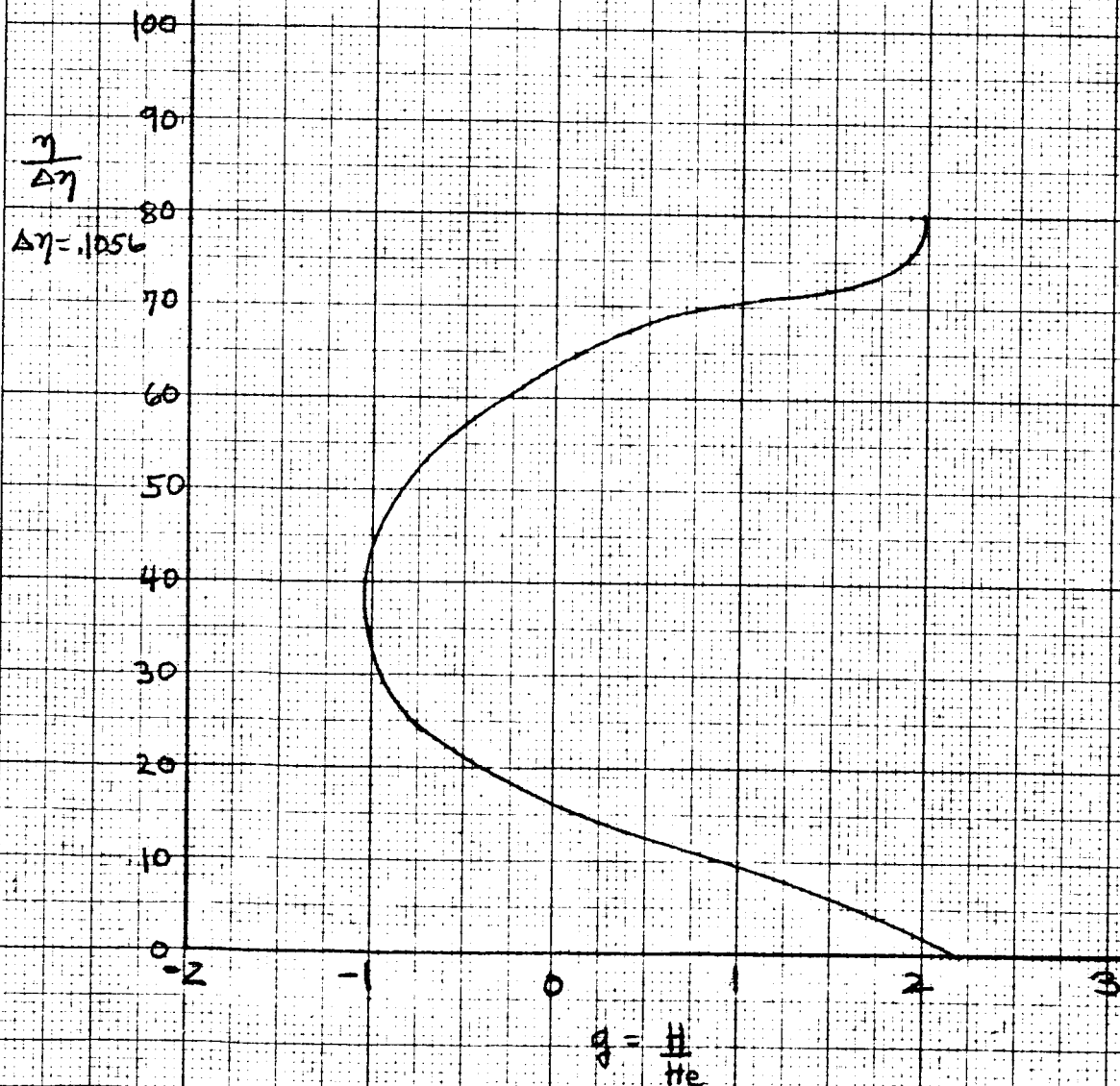


Figure 2c

Mass Fraction Distribution

$X = 3.40 \text{ ft}$

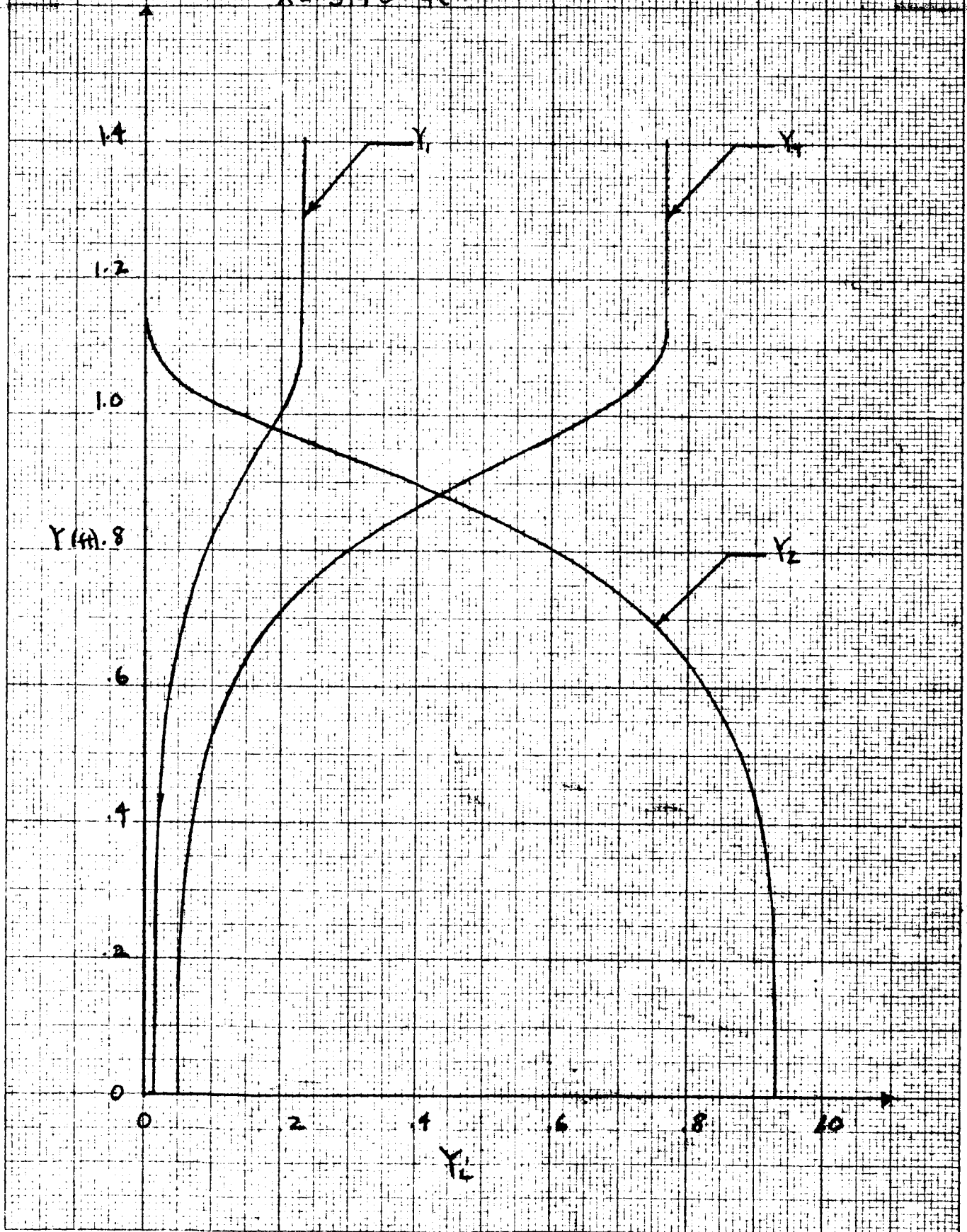


Figure 2d

Mass Fraction Distribution

$X = 17,000 \text{ ft}$

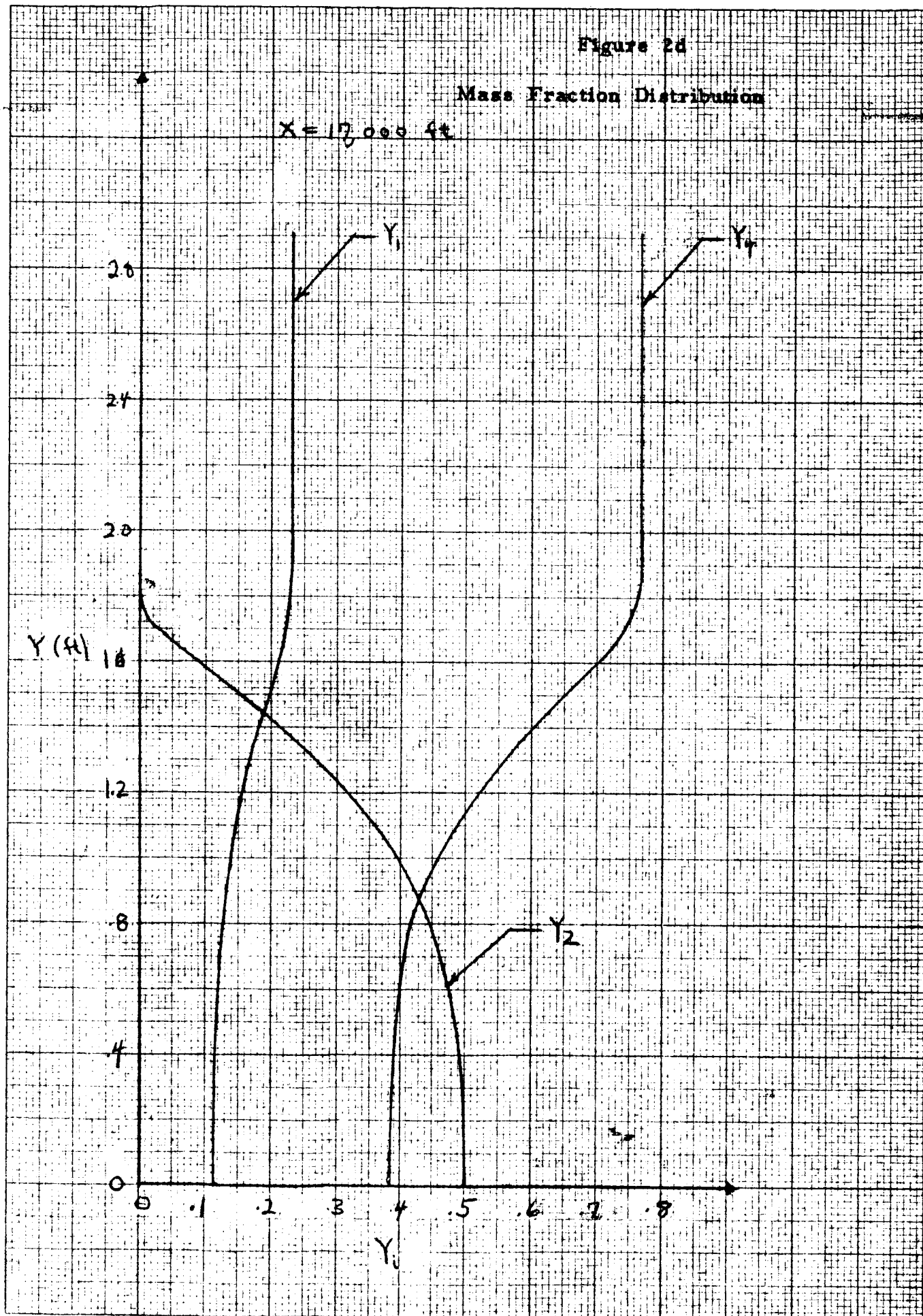
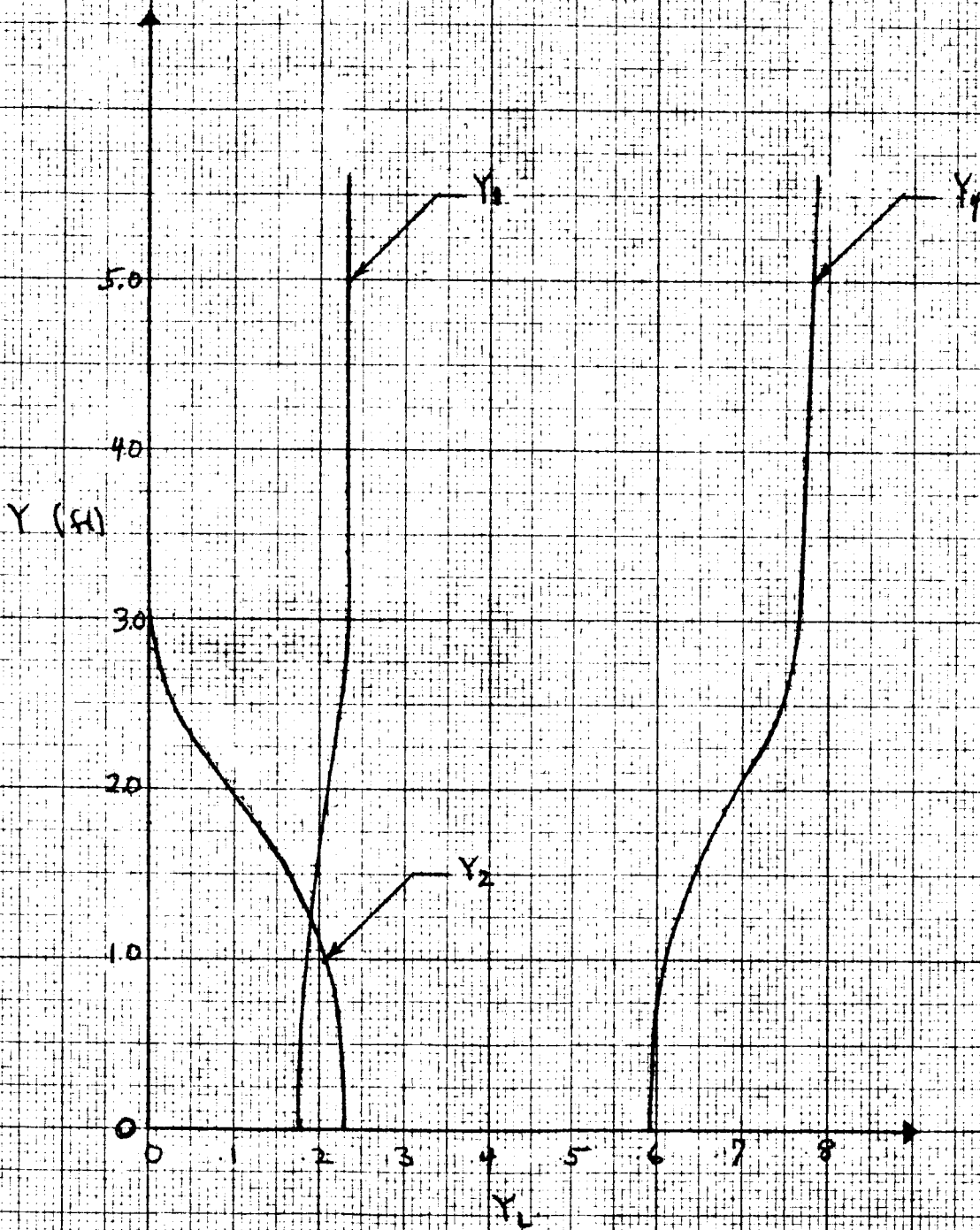


Figure 2e

Mass Fraction Distribution

$X = 49,000$ ft



40° back

5 11 19 72

Figure 2f

Static Temperature Distribution

X = 3140 ft

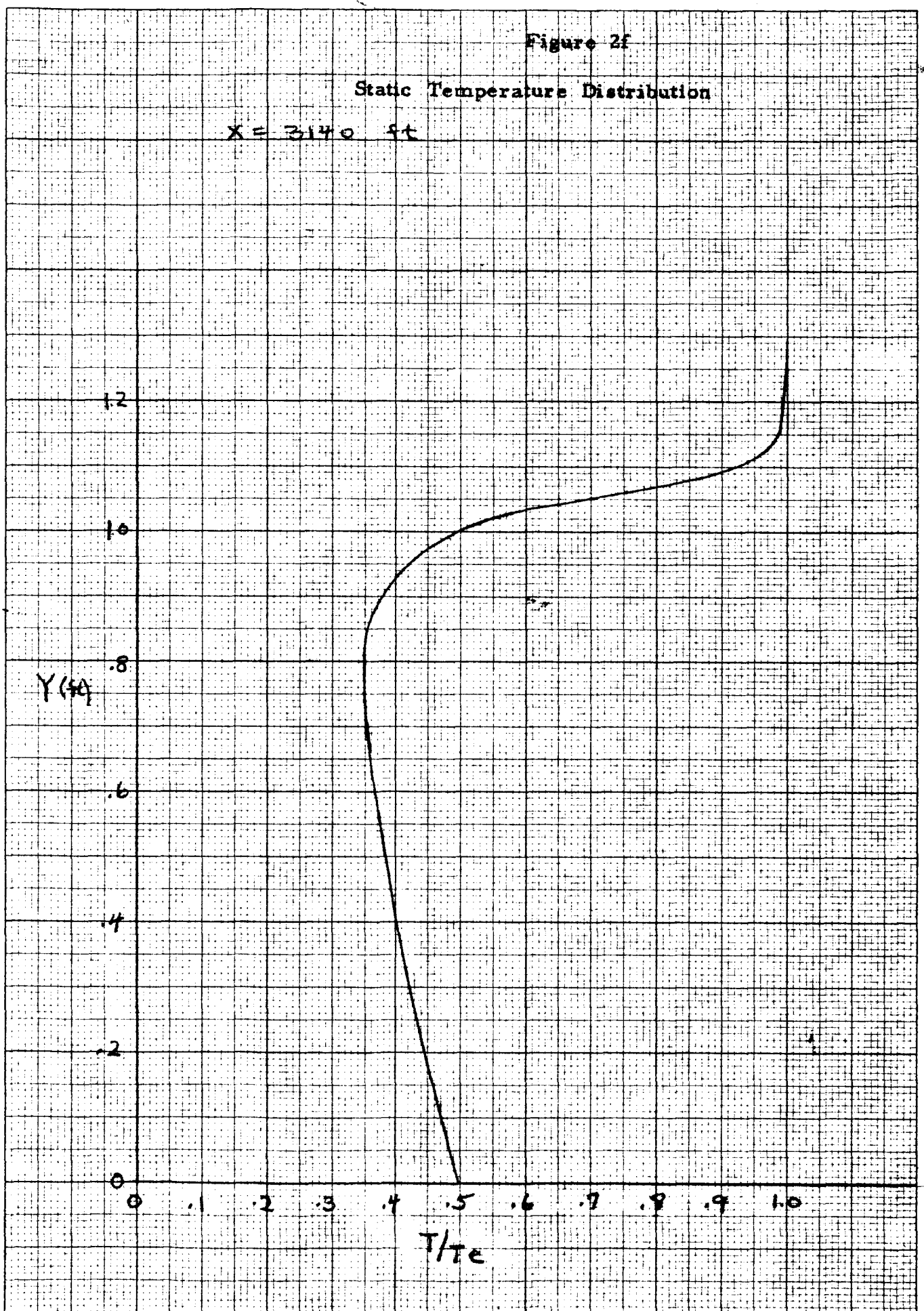


Figure 2g

Static Temperature Distribution

$X = 17,000$ ft

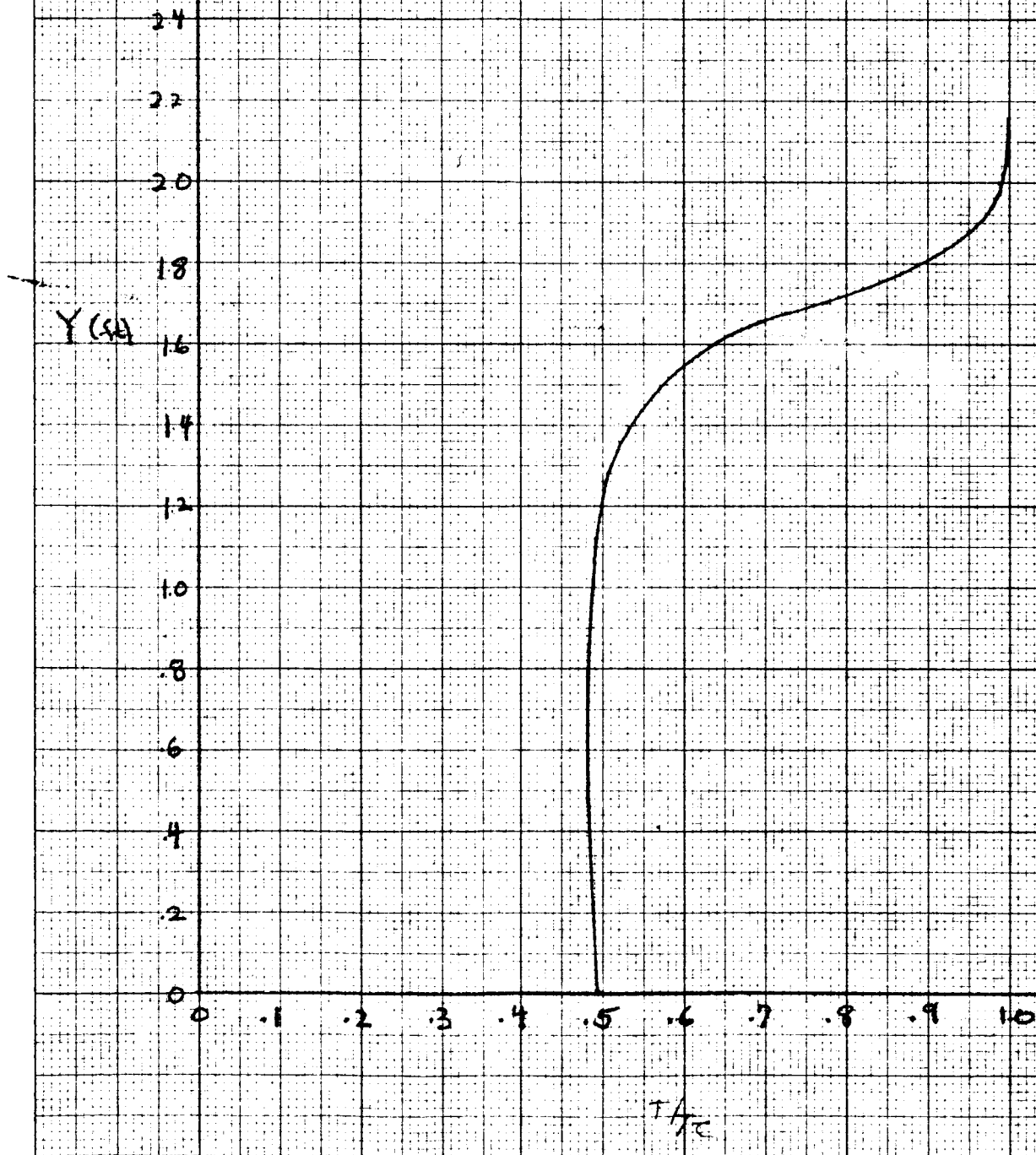
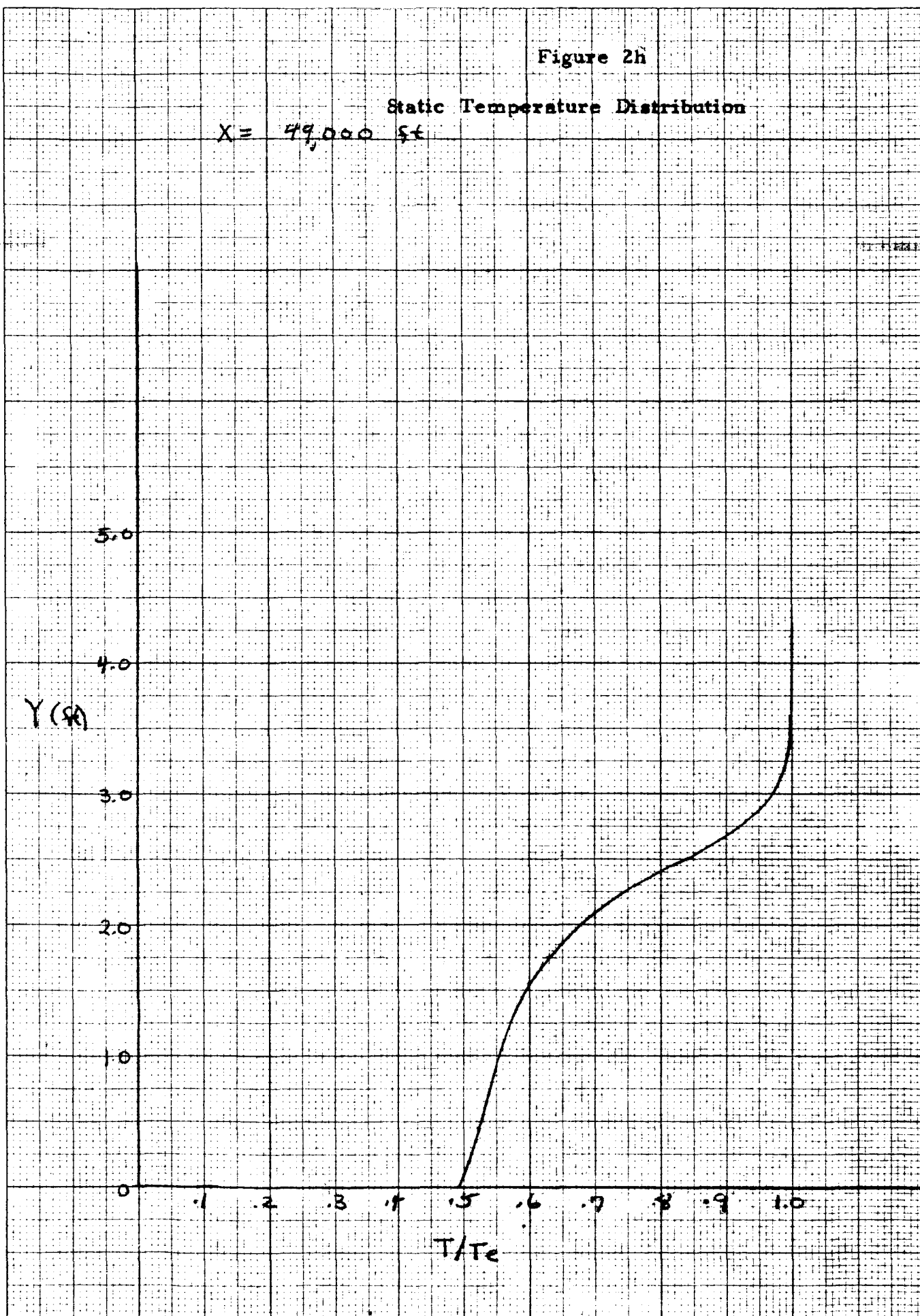
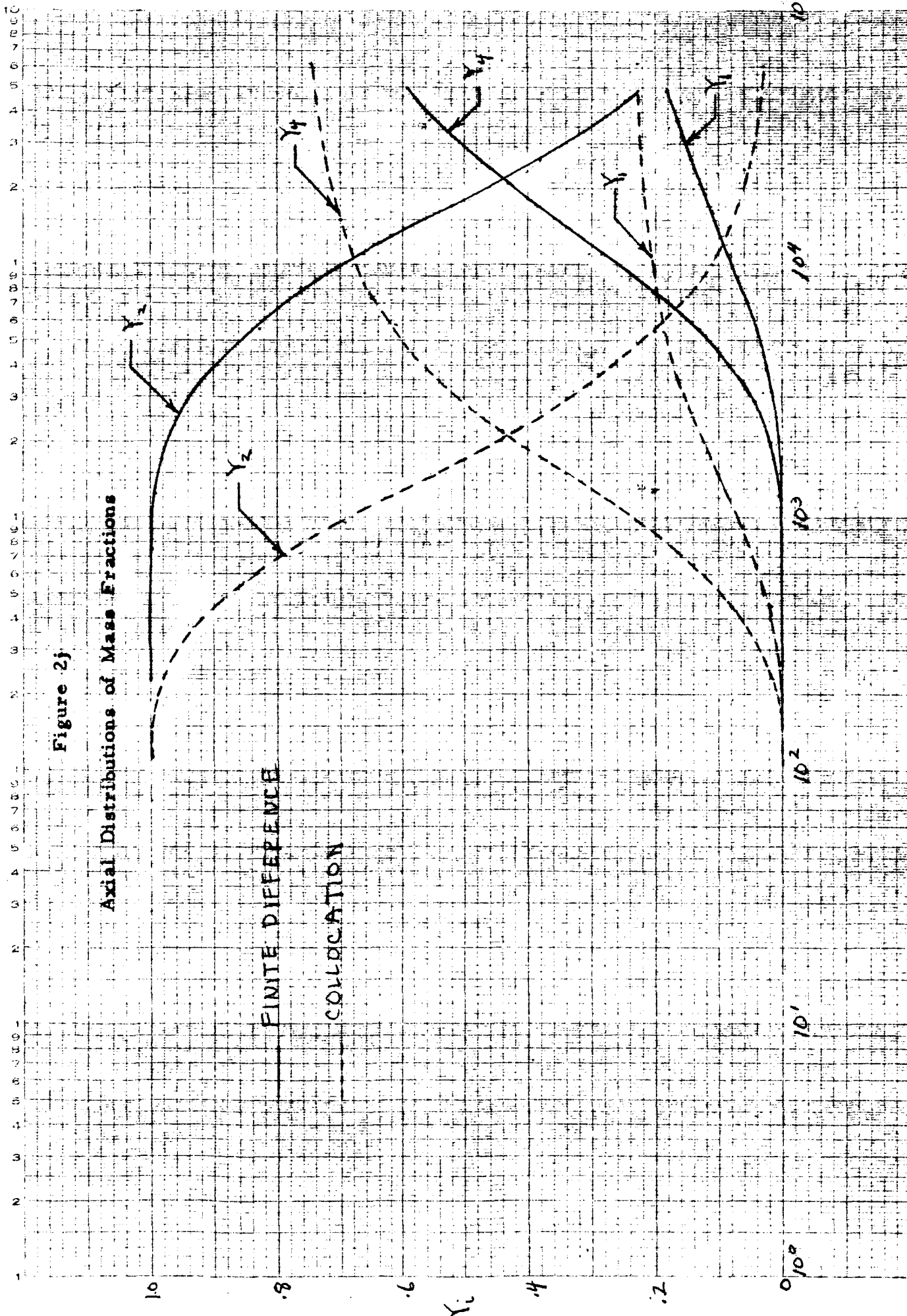


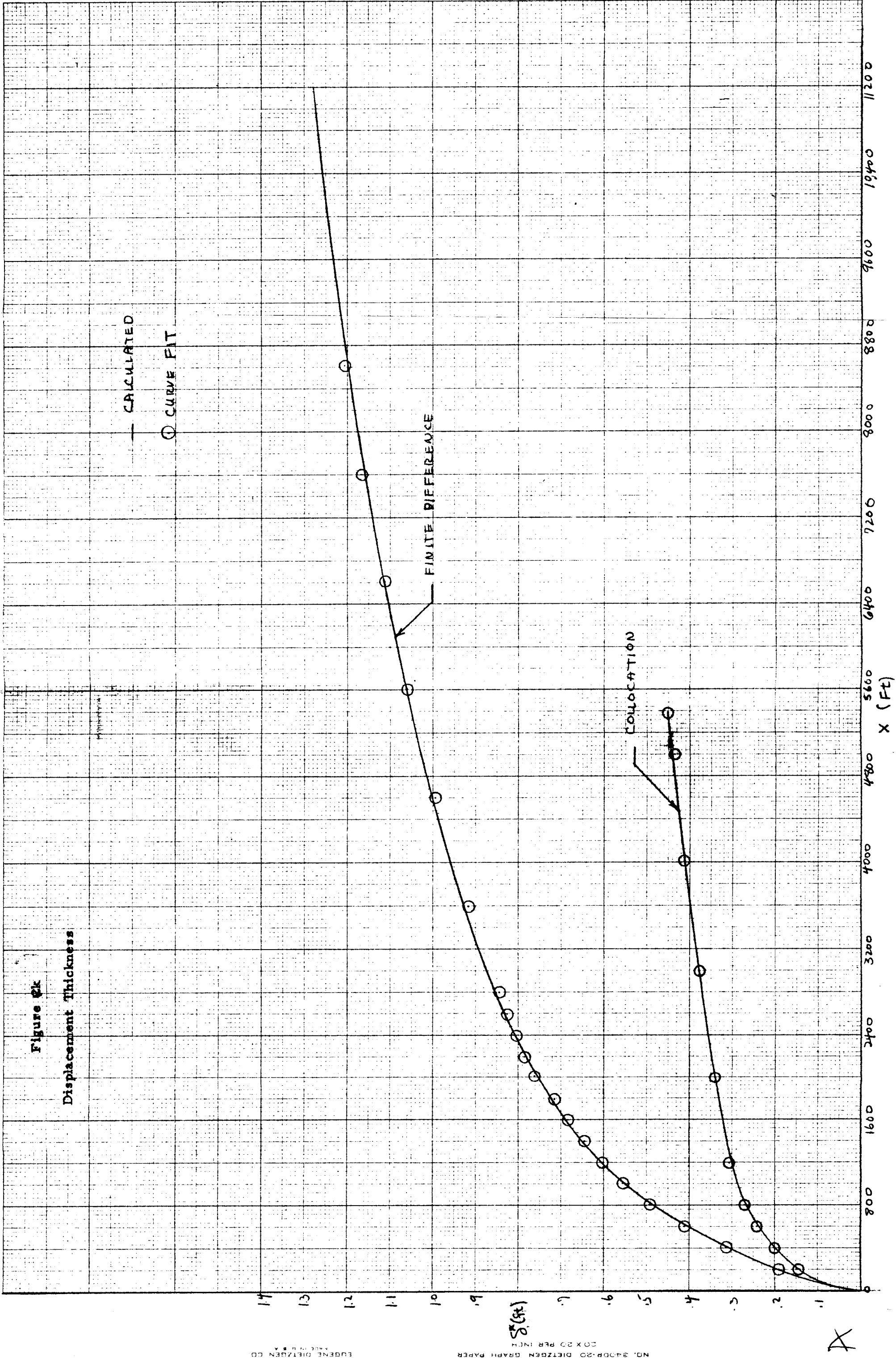
Figure 2h

Static Temperature Distribution

$X = 49,000 \text{ ft}$







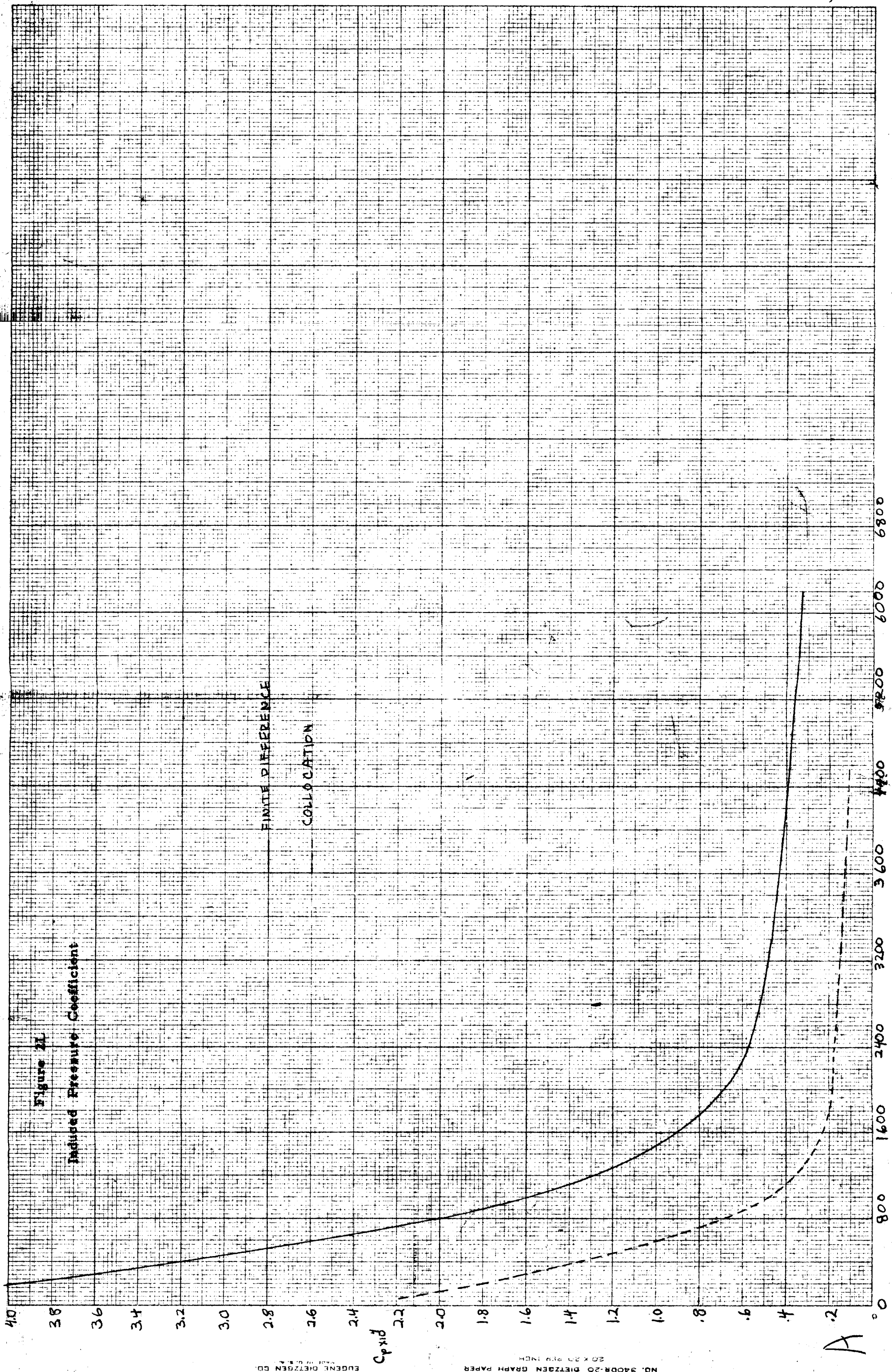


Figure 2L

Induced Pressure Coefficient

FINITE DIFFERENCE

COLLOCATION

C_{pi}

X (ft)

B

A

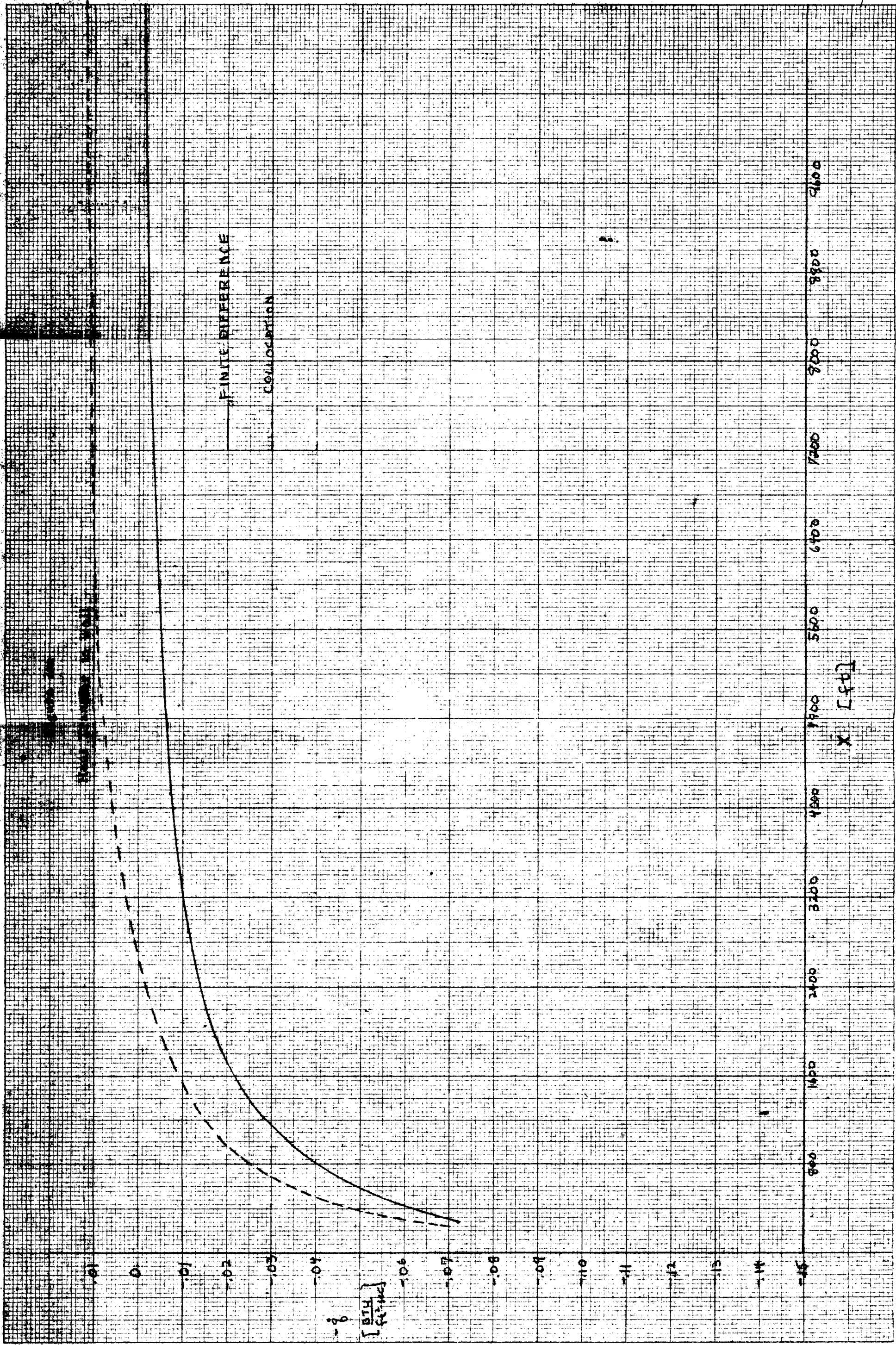
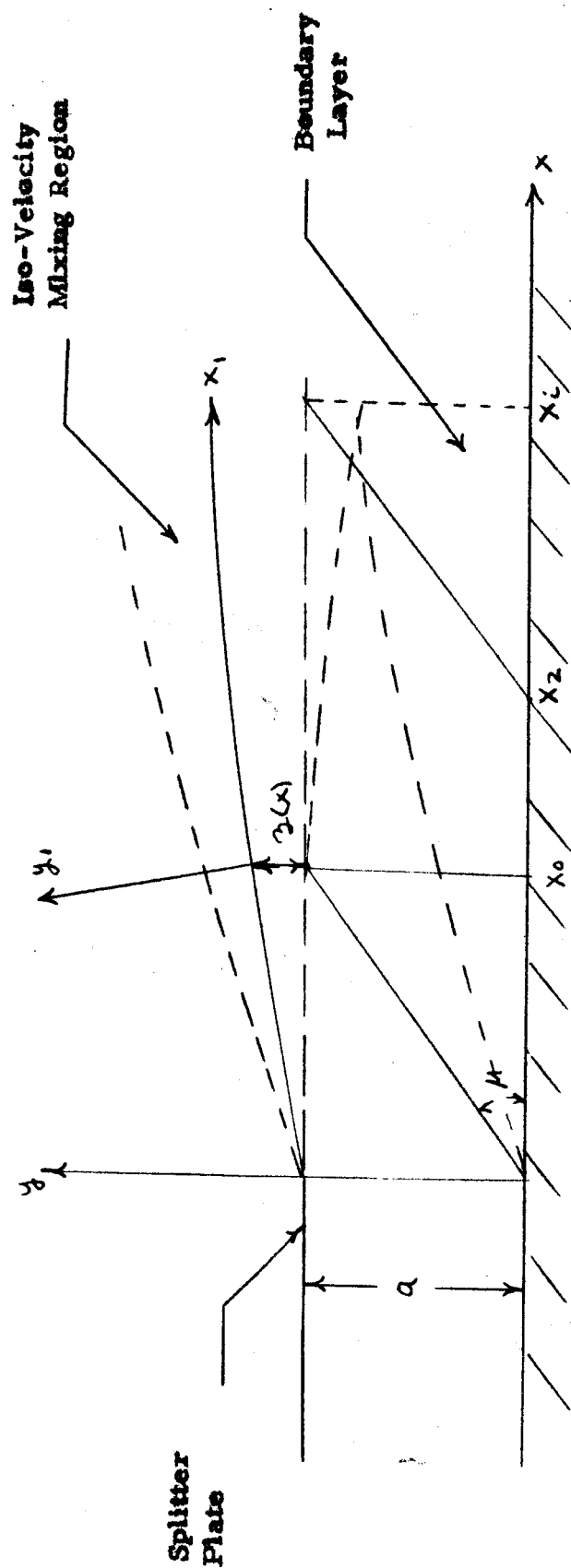


Figure 3

Slot Geometry



Initial Configuration

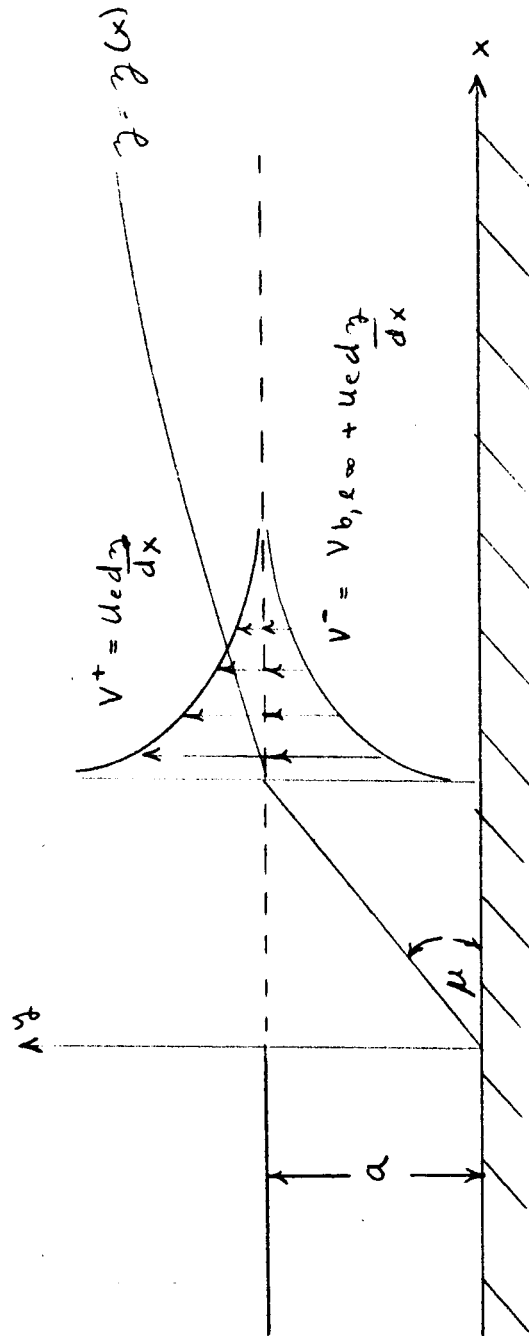


Figure 5

Finite Difference Scheme

